

SYMMETRIC RIBBON NUMBERS OF LOW-COMPLEXITY KNOTS

SAJID RAIHAN AKASH, ERIC CORRADO, BISHOP PLACKE, SAM SANKETH, NICK STARNES,
ANOK TIMOTHY, AND ALEXANDER ZUPAN

ABSTRACT. Every knot $K \subset S^3$ that admits a symmetric union presentation bounds an immersed ribbon disk in S^3 , while the converse is an open problem due to Christoph Lamm. The symmetric ribbon number $r_s(K)$ of K is the minimum number of ribbon singularities in any symmetric ribbon disk bounded by K . In this paper, we undertake a systematic investigation of symmetric ribbon numbers of knots with at most 12 crossings. Along the way, we exhibit novel lower bounds for $r_s(K)$ arising from knot determinants, Alexander polynomials, Jones polynomials, and Kauffman polynomials.

1. INTRODUCTION

In [Lam00], Lamm introduced the notion of a symmetric union presentation for a knot K , constructed by beginning with a symmetric diagram $D \# -D$ and inserting additional crossings along the axis of symmetry, as shown at left in Figure 1.

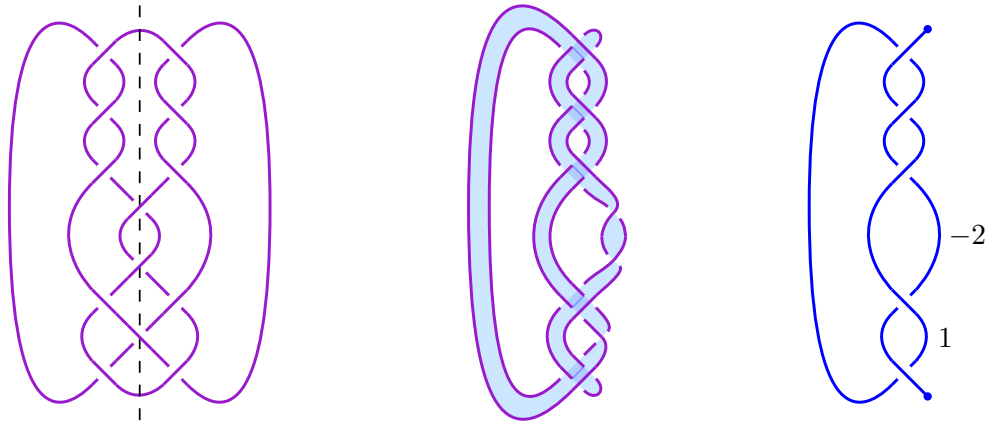


FIGURE 1. At left, a symmetric union presentation for the knot $12n_{313}$, appearing in [Lam21a]. At center, the corresponding symmetric ribbon disk, whose diagram can be obtained by “folding” the left picture in half across the axis of symmetry. At right, the symmetric ribbon disk is encoded as a *labeled knotoid diagram*.

Lamm observed that if K admits a symmetric union presentation, then K is a ribbon knot, posing the converse as a still-open question:

Question 1.1. *Does every ribbon knot admit a symmetric union presentation?*

Aceto reframed the idea of a symmetric union presentation by observing that every ribbon surface is isotopic to a “flattened” surface built from the pieces shown in Figure 2, proving that a ribbon disk \mathcal{D} arises from Lamm’s symmetric union construction if and only if \mathcal{D}

can be built without crossings or junctions [Ace14]. We call such a disk a *symmetric ribbon disk*, and a knot K is a *symmetric ribbon knot* if K bounds a symmetric ribbon disk. An example of a symmetric ribbon disk appears at center in Figure 1. Lamm showed that each of the 21 prime ribbon knots K with $c(K) \leq 10$ is symmetric ribbon knot [Lam00, Lam21b] and then proved the same for all but 15 of the 137 prime ribbon knots with crossing number 11 or 12 [Lam21a].

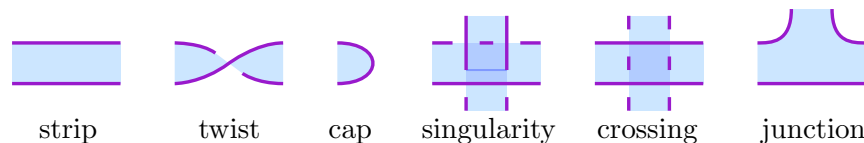


FIGURE 2. The fundamental pieces used to construct a modular ribbon disk.

For a ribbon knot K , the ribbon number $r(K)$ is defined to be the minimum number of ribbon singularities contained in any ribbon disk \mathcal{D} bounded by K . Ribbon number was introduced in [Miz06] and tabulated for prime knots up to 11 crossings in [FMZ24] and for prime knots with 12 crossings in [AAC⁺25]. Aceto defined the analogue for a symmetric ribbon knot K , the *symmetric ribbon number* $r_s(K)$, to be the minimum number of ribbon singularities in any symmetric ribbon disk bounded by K .

In this article, we explore various lower bounds for $r_s(K)$ arising from the determinant, Alexander polynomial, Jones polynomial, and Kauffman polynomial of a knot K . We apply our tool to low-complexity knots, proving

Theorem 1.2. *The symmetric ribbon numbers for all but 3 of the 44 known prime symmetric ribbon knots with 11 or fewer crossings appear in Table 2, the symmetric ribbon numbers for all but 4 of the 53 known prime nonalternating symmetric ribbon knots with crossing number 12 appear in Table 3, and the symmetric ribbon numbers for 27 of the 46 known prime alternating symmetric ribbon knots with crossing number 12 appear in Table 4.*

While it is clear from the definitions that $r(K) \leq r_s(K)$, our work yields the first examples of symmetric ribbon knots K such that $r(K) < r_s(K)$. Of the 105 prime symmetric ribbon knots up to 12 crossings such that both $r(K)$ and $r_s(K)$ are known, 56 satisfy $r(K) = r_s(K)$, 45 satisfy $r_s(K) - r(K) = 1$, and four, the knots $12a_{427}$, $12a_{435}$, $12a_{464}$, and $12a_{631}$, satisfy $r_s(K) - r(K) = 2$. Our data suggest several conjectures.

Conjecture 1.3. *For every positive integer n , there exists a symmetric ribbon knot K such that $r_s(K) - r(K) = n$.*

All of the knots in our data for which $r_s(K) - r(K) > 0$ have $r(K) \geq 3$. Thus, we also expect

Conjecture 1.4. *If K is a symmetric ribbon knot such that $r(K) = 2$, then $r_s(K) = 2$ as well.*

Note that Aceto proved for every n , there is a ribbon knot K_n such that $r(K_n) = 2$ while $r_s(K_n) > n$ [Ace14]. However, it is unknown whether the knots in Aceto's family are symmetric ribbon knots, and so this inequality admits the possibility that $r_s(K_n) = \infty$ (the convention for a ribbon knot that is not symmetric, should such a knot exist).

To determine the data referenced in Theorem 1.2 we encode symmetric ribbon disks as *labeled knotoid diagrams* (defined below, example shown at right in Figure 1) and employ

a number of different tactics. The first of our tools is the set of Alexander polynomials,

$$\mathfrak{R}_n^s = \{\Delta_K(t) : r_s(K) = n \text{ and } K \text{ is prime}\}.$$

A similar set, \mathfrak{R}_n , involving $r(K)$ was introduced in [FMZ24], in which the authors proved that \mathfrak{R}_n is finite for all n and determined the sets \mathfrak{R}_2 and \mathfrak{R}_3 . Since $\mathfrak{R}_n^s \subset \mathfrak{R}_n$, we have that \mathfrak{R}_n^s is also finite. We enumerate \mathfrak{R}_2^s and \mathfrak{R}_3^s in Lemmas 4.3 and 4.4 and prove

Theorem 1.5. *The set \mathfrak{R}_4^s consists of the 27 polynomials given in Table 1.*

If $r_s(K) = 5$, the set \mathfrak{R}_5^s is too large to compute via our methods. However, leveraging a Theorem of Kidwell about the z -degree of the Kauffman polynomial [Kid87], we obtain a restriction on these knots involving their determinants.

Theorem 1.6. *Suppose K is a prime symmetric ribbon knot. If $r_s(K) = 5$, then $\det(K) \leq 169$.*

Finally, we obtain additional restrictions via Jones polynomials. We show

Theorem 1.7. *Suppose K is a symmetric ribbon knot such that $r_s(K) = 2$, or $r_s(K) = 3$ and $\det(K) = 25$. Then there exists an integer n such that*

$$V_K(t) = (-t)^n \cdot f(t) + 1,$$

where

$$f(t) = -t^{-3} + t^{-2} - t^{-1} + 2 - t + t^2 - t^3 \text{ if } r_s(K) = 2$$

or

$$f(t) = t^{-4} - 2t^{-3} + 3t^{-2} - 4t^{-1} + 4 - 4t + 3t^2 - 2t^3 + t^4 \text{ if } r_s(K) = 3 \text{ and } \det(K) = 25.$$

Theorem 1.7 is a combination of Propositions 6.1 and 6.2, and it has both obstructive and constructive applications. For the knots

$$K \in \{11n_{39}, 12n_{256}, 12n_{257}, 12n_{394}, 12n_{870}\},$$

the Alexander polynomial $\Delta_K(t)$ is in \mathfrak{R}_3^s but not in \mathfrak{R}_2^s , so that the Alexander polynomial bound shows that $r_s(K) \geq 3$. However, $\det(K) = 25$ but $V_K(t)$ is not of the form of Theorem 1.7 (as shown in Corollary 6.3), and so we get the stronger bound $r_s(K) \geq 4$. On the other hand, for the knots $K = 11n_{37}$ or $12n_{414}$, symmetric union presentations from [Lam21a] indicate that $r_s(K) \leq 4$. Yet $\det(K) = 25$ and $V_K(t)$ satisfies the conclusion of Proposition 6.2, which contains a stronger statement and indicates precisely where to look to find a symmetric ribbon disk for K with three ribbon intersections, should it exist. Via experiment, we found the new symmetric union disks depicted in Figure 3, verifying that $r_s(K) = 3$ for these two knots. More details are included in Remark 6.4.

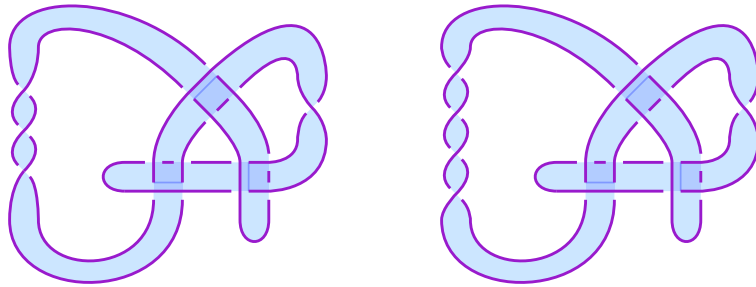


FIGURE 3. Symmetric ribbon disks for $11n_{37}$ (left) and $12n_{414}$ (right).

Our work relied heavily on computations performed using SnapPy [CDGW] within SageMath [The21] and the knot data available through KnotInfo [LM26].

1.1. Organization. In Section 2, we set up preliminaries, including the process of converting a labeled knotoid diagram to a symmetric ribbon disk and vice versa, along with moves on labeled knotoid diagrams. In Section 3, we classify singular arc diagrams (knotoid diagrams without crossing information) with two, three, and four crossings. In Section 4, we determine the sets \mathfrak{R}_2^s and \mathfrak{R}_3^s and include Table 1. In Section 5, we prove Theorem 1.6, and in Section 6, we prove Theorem 1.7. Finally, we use all of our tools to tabulate symmetric ribbon numbers for prime knots up to 12 crossings within the tables in Section 7. Section 8 is an appendix in which we complete the proof of Theorem 1.5.

1.2. Acknowledgments. We thank the College of Arts and Sciences at the University of Nebraska-Lincoln for running the three-week course MATH 391: Special Topics in Mathematics in January 2024, during which this project was first conceived and initiated. NS was supported by UNL's Undergraduate Creative Activity and Research Experience (UCARE) program during summer 2024, and AT was supported by the UCARE program during academic year 2024-2025. AZ thanks Dimos Goundaroulis for enlightening communications about the tabulation of knotoid diagrams and Jeffrey Meier for helpful conversations about ribbon knots and disks. AZ was supported in part by NSF grant DMS-2405301 and a Simons Travel Support award.

2. PRELIMINARIES

We work in the smooth category throughout. A knot $K \subset S^3$ is called *ribbon* if K bounds an immersed disk $\mathcal{D} \subset S^3$ with only ribbon singularities, called a *ribbon disk* for K . The *ribbon number* $r(\mathcal{D})$ counts the number of ribbon singularities contained in \mathcal{D} , and the *ribbon number* $r(K)$ of K is defined as

$$r(K) = \min\{r(\mathcal{D}) : \mathcal{D} \text{ is a ribbon disk for } K\}.$$

If K is non-trivial, then $r(K) \geq 2$ (see [FMZ24, Remark 2.7], for instance). Every ribbon disk \mathcal{D} can be flattened to a projection plane and built from six types of fundamental pieces, shown in Figure 2: Caps, strips, crossings, singularities, crossings, and junctions. These pieces were discussed in [Eis09], and [Ace14], and if a ribbon disk \mathcal{D} is realized as a union of these building blocks, we call \mathcal{D} a *modular ribbon disk*.

A symmetric union presentation D^* , introduced in [Lam00], is defined as follows: First, start with a knot diagram D for a knot J . The diagram $D \# -D$, which we call the *initial diagram*, has an axis of symmetry ℓ . Choose some number of pairwise disjoint disks $\Delta_1, \dots, \Delta_k$ which have reflection symmetry over ℓ and such that each disk Δ_i meets $D \# -D$ in a pair of arcs that also have reflection symmetry over ℓ . Now, replace each $(D \# -D) \cap \Delta_i$ with a tangle diagram T_i so that all crossings of T_i occur on the axis of symmetry ℓ . The resulting diagram D^* is called a *symmetric union presentation with partial knot J* . Lamm proved that if K admits a symmetric union presentation with partial knot J , then K is a ribbon knot and $\det(K) = (\det(J))^2$ [Lam00]. See Figure 1 for an example of a symmetric union presentation.

Related to modular diagrams, Aceto proved a useful proposition:

Proposition 2.1. [Ace14] *A knot $K \subset S^3$ admits a symmetric union presentation if and only if K bounds a modular ribbon disk \mathcal{D} that contains no crossings or junctions.*

In light of Proposition 2.1, a modular ribbon disk \mathcal{D} without crossings or junctions is called *symmetric ribbon disk*, and a knot K bounding a symmetric ribbon disk is called a

symmetric ribbon knot. Aceto naturally defined the *symmetric ribbon number* $r_s(K)$ of a symmetric ribbon knot to be

$$r_s(K) = \min\{r(\mathcal{D}) : \mathcal{D} \text{ is a symmetric ribbon disk for } K\}.$$

Immediately, we have

Lemma 2.2. $r_s(K) \geq r(K)$.

Lamm’s work in [Lam00] and [Lam21a] contains a number of symmetric union presentations for knots. To find upper bounds on the symmetric ribbon numbers of these knots, we describe a method for converting a symmetric union presentation to a labeled knotoid diagram. A *knotoid diagram* κ is an immersed arc in S^2 with only double points, in which each double point is endowed with crossing information. We call the endpoints of the arc the *aglets* of κ . The n crossings cut κ into $n + 1$ connected arcs called *strands*, and a *labeled knotoid diagram* is a knotoid diagram with each strand labeled with an integer.

Lemma 2.3. *Every symmetric union presentation induces a labeled knotoid diagram, and vice versa.*

Proof. Suppose that K admits a symmetric union presentation D^* with partial knot J and initial diagram $D\# -D$. Cut $D\# -D$ along its axis of symmetry ℓ , yielding two arcs, and interpret one of these arcs as a knotoid diagram κ . Note that κ meets each of the disks $\Delta_1, \dots, \Delta_k$ in the definition of a symmetric union presentation. For each strand of κ , label it with the sum of the (signed) number of crossings contained in all disks $\Delta_1, \dots, \Delta_k$ that the strand meets.

Conversely, we can convert a labeled knotoid diagram κ to a symmetric ribbon disk: First, we ignore the labeling of κ , convert each aglet to a cap, convert each arc to a strip, and convert each crossing to a singularity, as shown below in Figure 4. Note that there are two different choices of singularity corresponding to each crossing. We can make either choice, provided that our choices are *globally consistent*, meaning that we can traverse our diagram from one cap to the other so that every time we pass through a singularity, we travel through two over-crossings (corresponding to an under-crossing in κ) or we travel through an over- and under-crossing (corresponding to an over-crossing in κ). If our choices are globally consistent, this process produces a diagram of the form $D\# -D$. Finally, we add in twists (with signs) corresponding to the labelings to complete the process. By Proposition 2.1, this symmetric ribbon disk induces a symmetric union presentation. \square

An example of the process of converting a symmetric union presentation to a labeled knotoid diagram is shown in Figure 1. An example of the reverse process, converting a labeled knotoid diagram to a symmetric ribbon disk, is carried out in Figure 4. By convention, 0-labelings are omitted.

Given a knotoid diagram κ , the *closure* of κ , denoted $\text{cl}(\kappa)$, is the knot corresponding to a diagram obtained by connecting the aglets of κ with an arc that contains only over-crossings.

Lemma 2.4. *If K admits a symmetric union presentation inducing labeled knotoid diagram κ , then $\det(K) = (\det(\text{cl}(\kappa)))^2$.*

Proof. This follows immediately from [Lam00] and the observation that $\text{cl}(\kappa)$ is a diagram for the partial knot J corresponding to the symmetric union presentation. \square

Given two knotoid diagrams κ' and κ'' , we can form the *knotoid connected sum* $\kappa' \# \kappa''$ by removing small disk neighborhood of one aglet from each diagram and gluing along the resulting boundary curves. Note that the connected sum may depend on our choices of

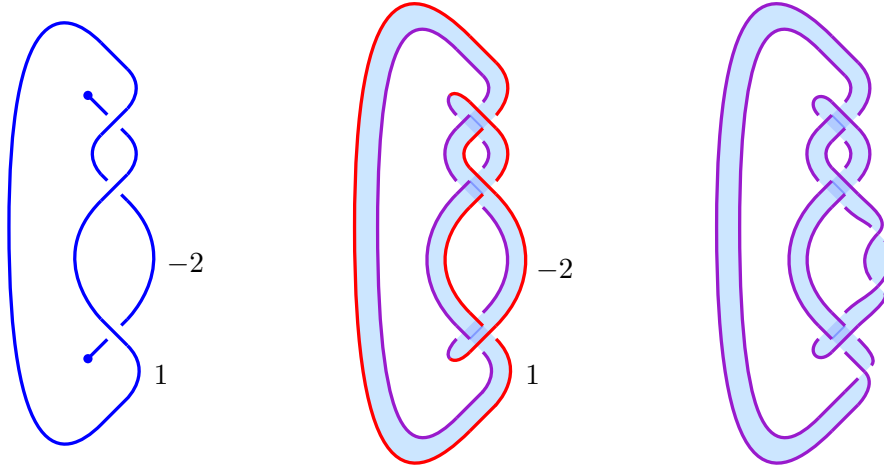


FIGURE 4. Converting a labeled knotoid diagram to a symmetric ribbon disk. In the middle, the red path traverses the diagram in a way that satisfies the global consistency condition (it never passes through a singularity with two under-crossings). Note further that the knotoid diagram at left is equivalent to the one in Figure 1.

aglets. Conversely, a knotoid diagram κ is called *composite* if there exists a simple closed curve c meeting κ once and cutting S^2 into two disks such that each contains at least one crossing. In this case, c can be used to realize κ as $\kappa' \# \kappa''$. If the diagram κ is not composite, we say that κ is *prime*. See Figure 5 for an example.

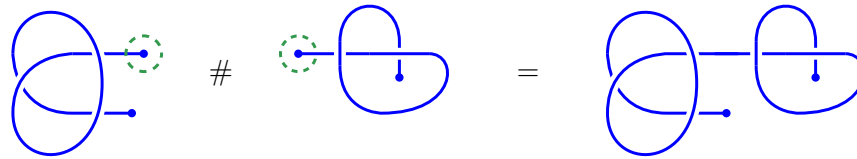


FIGURE 5. An example of the connected sum operation on knotoid diagrams.

Near the aglet, we note several simplifications. First, the strand connected to the aglet need not be labeled, since any labeling yields twisting on the induced symmetric ribbon disk that can be eliminated via isotopy, as shown in Figure 6. In addition, by construction we have that if a labeled knotoid diagram κ induces a symmetric ribbon disk \mathcal{D} , then $r(\mathcal{D}) = c(\kappa)$, where $c(\kappa)$ is the crossing number of κ . If the strand leaving the aglet meets an over-crossing of κ , we may eliminate the corresponding singularity via isotopy, inducing the move shown in Figure 7, which we call an *aglet move*.

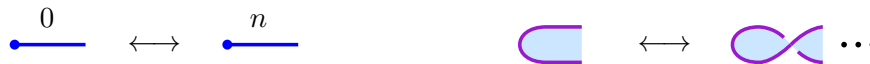


FIGURE 6. The labeling of the strand adjacent to the aglet can be changed via isotopy, and so we generally assume this strand is labeled zero.



FIGURE 7. If the strand adjacent to an aglet meets an over-crossing of κ , we may eliminate the crossing (and its corresponding singularity) via an aglet move.

It may be possible to simplify a given labeled knotoid diagram by performing Reidemeister moves. For example, if a knotoid diagram κ admits an R1 move, then the corresponding symmetric ribbon disk can be simplified by eliminating a singularity, as shown in Figure 8. For an R2 move, the situation is more complicated. We can perform an R2 move to simplify the a labeled knotoid diagram if and only if the strand adjacent to both under-crossings has label zero, as shown in Figure 9. Similarly, an R3 move can be performed only when the strand adjacent to two under-crossings has label zero, as shown in Figure 10.



FIGURE 8. An R1 move on a labeled knotoid diagram translates to a move on the corresponding symmetric ribbon disk. Labelings change as shown.

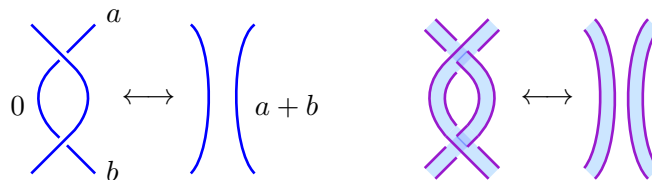


FIGURE 9. An R2 move on a labeled knotoid diagram translates to a move on the corresponding symmetric ribbon disk. The strand shown at left must be labeled zero for this move to be possible.

If two labeled knotoid diagrams κ and κ' are related via a sequence of aglet moves, R1 moves, R2 moves, R3 moves, and planar isotopy, we say that κ and κ' are equivalent. We have demonstrated that if κ and κ' are equivalent, then they induce symmetric ribbon disks \mathcal{D} and \mathcal{D}' such that $\partial\mathcal{D}$ and $\partial\mathcal{D}'$ are isotopic knots. As an example, the labeled knotoid diagrams in Figures 1 and 4 are equivalent. Note that neither labeled knotoid diagram admits a simplifying R2 move, since the requisite strand has label -2 (not zero). The symmetric ribbon disk in Figure 4 illustrates how nonzero twisting obstructs the isotopy shown in Figure 9.

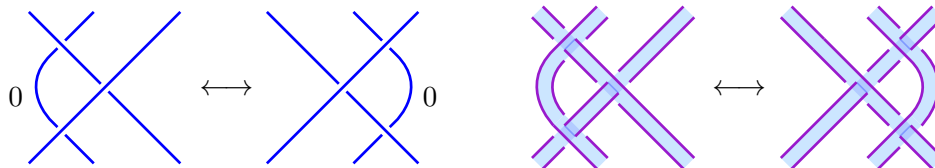


FIGURE 10. An R3 move on a labeled knotoid diagram translates to a move on the corresponding symmetric ribbon disk. The strand shown at left must be labeled zero for this move to be possible.

Remark 2.5. Our construction differs slightly from that in [Lam21a] in our conventions reverse the signs of the crossings in the corresponding knotoid diagrams. The reason for this change involves the labeling of strands. With Lamm’s conventions, two different labels may be needed on opposite sides of an over-crossing, while a label can be passed through an under-crossing. For our conventions, twisting can be passed through over-crossings (but not under-crossings), and so it is enough to label each connected strand. See Figure 11.

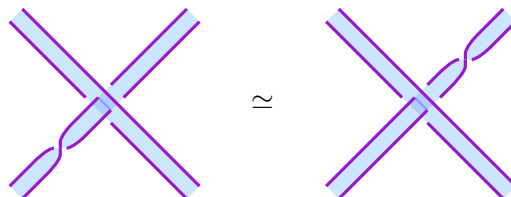


FIGURE 11. Twisting on the strip corresponding to an over-crossing of a labeled knotoid diagram can be pushed to either side of the associated singularity.

We can use labeled knotoid diagrams to obtain upper bounds for symmetric ribbon numbers. Proposition 2.6 already appears as Lemma 2.1 in [FMZ24], but we include another proof here using labeled knotoid diagrams.

Proposition 2.6. *Suppose that K admits a symmetric union presentation with initial diagram $D \# -D$ and axis of symmetry ℓ . If there are n consecutive over-crossings (or n consecutive under-crossings) in D adjacent to ℓ , then K bounds a symmetric ribbon disk \mathcal{D} such that $r(\mathcal{D}) = c(D) - n$.*

Proof. If there are n consecutive over-crossings adjacent to ℓ , then the induced labeled knotoid diagram κ admits a total of n simplifying aglet moves, inducing a symmetric ribbon disk \mathcal{D} with $c(D) - n$ singularities, so that $r(\mathcal{D}) = c(D) - n$. In the case of n consecutive under-crossings, we perform an involution of S^3 to convert the under-crossings to over-crossings and repeat the argument. \square

The example in Figure 1 has two over-crossings adjacent to its axis of symmetry, while $c(D) = 5$. Thus, aglet moves (carried out in Figure 4) yield a labeled knotoid diagram with three crossings, in turn yielding a symmetric ribbon disk with ribbon number three.

3. CLASSIFYING REDUCED SINGULAR ARC DIAGRAMS WITH AT MOST FOUR CROSSINGS

To tabulate symmetric ribbon numbers, we wish to understand all possible symmetric ribbon disks with ribbon number up to four, and by our work in Section 2, it suffices to understand labeled knotoid diagrams with at most four crossings. Although it would be a convenient shortcut to appeal to existing knotoid classifications (see [GDS19], for example), R2 and R3 moves are not allowed in our setting, and so our notion of knotoid equivalence is different from what usually appears in the literature. To understand knotoid diagrams within our framework, we first consider a knotoid diagram without crossing information, which we call a *singular arc diagram*, an immersed arc in S^2 with double points, considered up to planar isotopy. A crossing of a singular arc diagrams is said to be *incident* to an aglet if the aglet is connected to the crossing via an embedded arc. To carry out an exhaustive search for low-crossing singular arc diagrams, we eliminate diagrams that admit obvious simplifications. A singular arc diagram λ is *reduced* if

- (1) λ does not contain an embedded arc meeting the same crossing in two points,
- (2) if c is a simple closed curve meeting λ in a single point, then c bounds a disk containing an aglet and no crossings, and
- (3) no crossing is incident to both aglets.

If λ is unreduced, then any corresponding labeled knotoid diagram admits a simplifying R1 move (if (1) fails), any corresponding knotoid diagram is not prime (if (2) fails), or any corresponding labeled knotoid diagram admits a simplifying aglet move (if (3) fails).

Given a reduced singular arc diagram λ , we call a crossing incident to an aglet an *aglet crossing* and any crossing that is not an aglet crossing an *interior crossing*. In addition, we call the arc leaving an aglet crossing opposite the aglet an *aglet arc*. Note that a reduced singular arc diagram λ will have exactly two aglet crossings, and the two aglet arcs will not connect (otherwise λ is an immersion of the disjoint union of an arc and a curve, in which case we say λ is *disconnected*).

Lemma 3.1. *Up to symmetry, there is one reduced singular arc diagram with two crossings, 2_1 , shown at right in Figure 12.*

Proof. Suppose λ is a reduced singular arc diagram with $c(\lambda) = 2$ and consider the aglet arc of one of the aglet crossings. The aglet arc must connect to a non-aglet arc, and up to symmetry, this connection can be accomplished in only one way, as shown at left in Figure 12. Since λ is reduced, all remaining arcs must connect the two distinct crossings, and in S^2 , there is a unique way to make such connections up to isotopy, shown at right in Figure 12. \square

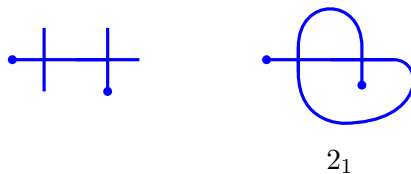


FIGURE 12. At left, an arc must connect the two aglet crossings of a reduced singular arc diagram λ with $c(\lambda) = 2$. At right, completing the diagram to get λ , which we call 2_1 .

Moving to crossing number three is only slightly more complicated.

Lemma 3.2. *Up to symmetry, there are two reduced singular arc diagrams with three crossings, 3_1 and 3_2 , shown at bottom left and bottom middle in Figure 13.*

Proof. Let λ be a reduced singular arc diagram with $c(\lambda) = 3$. A total of five arcs connect the three crossings, and since the interior crossing of λ must meet exactly four of these arcs, there must be one arc connecting the aglet crossings (and this arc cannot be the aglet arc for both crossings). Up to symmetry, there are three possible ways to connect the two aglet crossings via an arc, shown at top in Figure 13. Since all four remaining arcs must connect to the interior crossing, each configuration at top can be uniquely completed (up to isotopy) to a possible singular arc diagram λ , shown at bottom in Figure 13. However, the bottom right diagram is disconnected, leaving only the two possibilities at bottom left and middle. \square

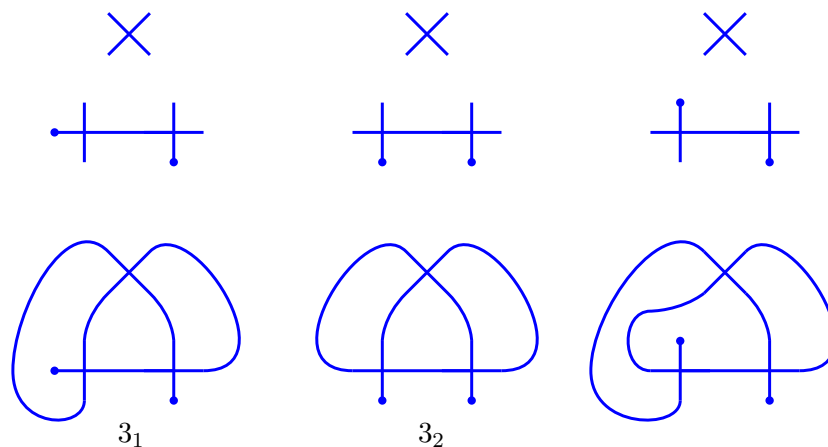


FIGURE 13. At top, possible connections between aglet crossings. At bottom, completing the diagrams. Note that only the bottom left (3_1) and middle (3_2) are valid, since the bottom right diagram is disconnected.

The case that $c(\lambda) = 4$ requires significantly more work.

Proposition 3.3. *Up to symmetry, there are eight reduced singular arc diagrams with four crossings, $4_1, 4_2, 4_3, 4_4, 4_5, 4_6, 4_7$, and 4_8 , shown in Figure 14.*

Proof. Let λ be a reduced singular arc diagram with $c(\lambda) = 4$, so that λ contains two aglet crossings and two interior crossings, which are connected by a total of seven arcs. We break the classification of λ into cases, depending on whether there are zero, one, or two arcs connecting the aglet crossings of λ .

Case A: Suppose that λ contains two arcs connecting the aglet crossings. Then two arcs must connect aglet crossings to interior crossings, which leaves three arcs connecting interior crossings. However, it is impossible to connect interior crossings with three arcs without creating a closed loop, resulting in λ being disconnected, a contradiction.

Case B: Suppose that λ contains one arc connecting the aglet crossings. The three possible configurations for this connection are shown at top in Figure 13. In each of these three configurations, we know that each of the six remaining arcs must be connected to at least one interior crossing, and so we connect one of the aglet arcs to an interior crossing, as shown in Figure 15. Of the five remaining arcs, four must connect to the additional

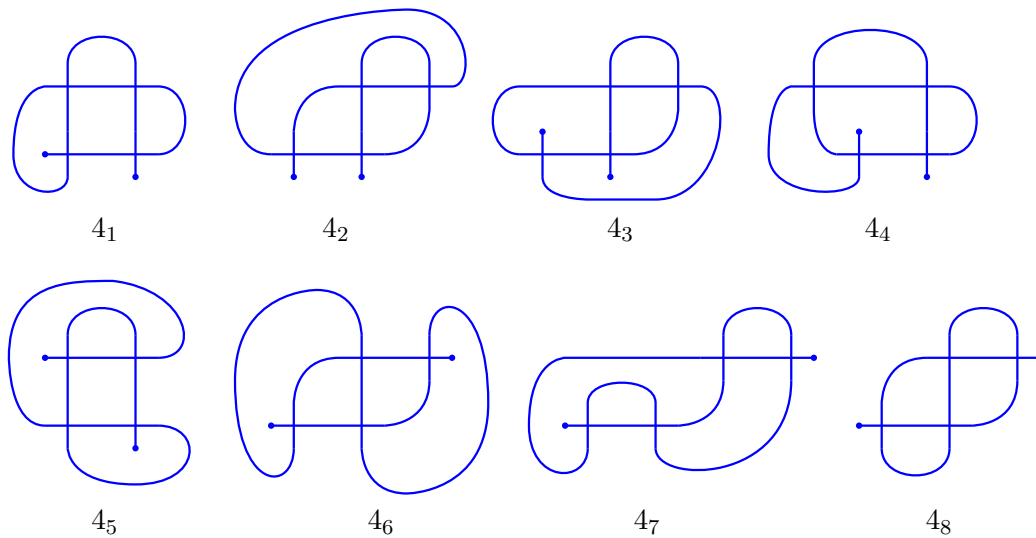


FIGURE 14. The eight possible reduced singular arc diagrams with four crossings.

interior crossing and one does not, with both endpoints connected to one of the structures shown in Figure 15. For each of the three structures, we first add this additional arc without introducing extra components, separating the remaining connections, forcing λ to be unreduced, or adding a second arc connecting aglet crossings, after which there is a unique way to add the second interior crossing and the four arcs connected to it.

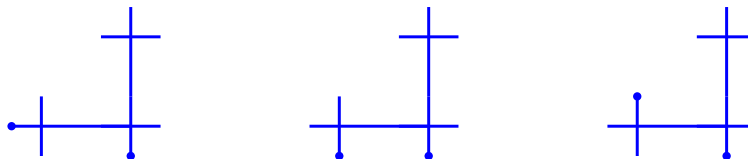


FIGURE 15. The three structures from Figure 13 with an additional interior crossing attached to an aglet arc.

For the first structure, there are two admissible ways to add an arc, shown at top in Figure 16. Once the additional arc is added, we can uniquely add the other interior crossing and four remaining arcs, shown at bottom in Figure 16. Note that one of the completions is disconnected.

With the second structure, there are two valid ways to add this additional arc, shown at top in Figure 17, and then each diagram can be uniquely completed with an additional interior crossing and four connecting arcs, shown at bottom in Figure 17. As above, one of these completions is disconnected. With the third configuration, there are two admissible ways to add the additional arc, shown at top in Figure 18, and both of the completions are valid, shown at bottom in the same figure.

Case C: Suppose that λ contains no arcs connecting the aglet crossings. Then all arcs connected to an aglet crossing are also connected to an interior crossing. There are several sub-cases to consider. First, suppose that the aglet arcs are connected to the same interior

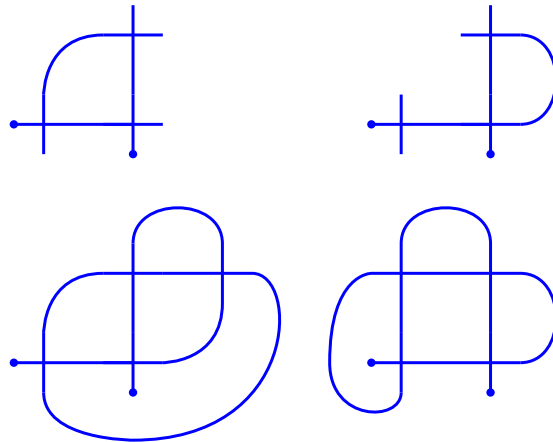


FIGURE 16. At top, the addition of one arc to the first structure. At bottom, completing the diagrams by including another interior crossing and four more arcs. The completion at bottom left is disconnected, so we disregard it.

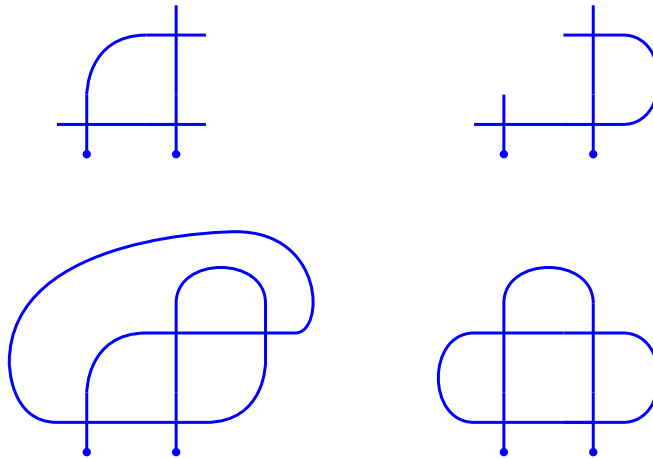


FIGURE 17. At top, the addition of one arc to the second structure. At bottom, the completions, where the one at right is disconnected.

crossing. Unless λ is disconnected, there is a unique configuration, shown at left in Figure 19. Of the five remaining arcs, four are connected to the other interior crossing, and so one more connects an aglet crossing to the first interior crossing. Up to symmetry, there is only one way to add this arc without disconnecting the other connections, adding another arc connecting aglet crossings, or forcing λ to be unreduced, shown at middle in Figure 19, and then the second interior crossing and connecting arcs are completed uniquely up to isotopy, shown at right in Figure 19.

Next, suppose that the aglet arcs are connected to different interior crossings. Then five more arcs must be added to the diagram at left in Figure 20. Suppose first that no additional arcs connect the top aglet crossing to the top interior crossing. Then two arcs connect the top aglet crossing to the bottom interior crossing, and two arcs connect the

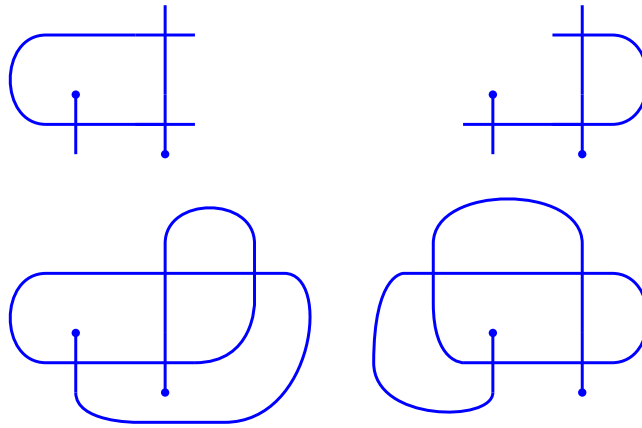


FIGURE 18. At top, the addition of one arc to the third structure. At bottom, both completions are valid.

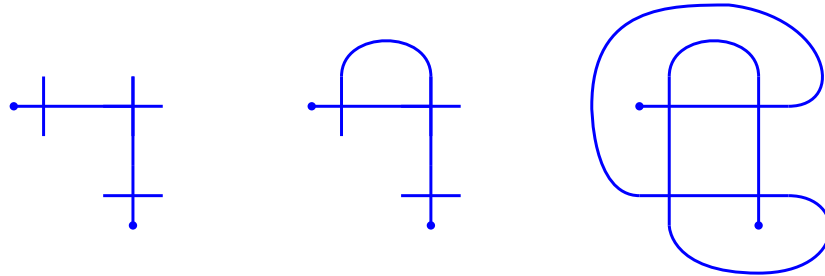


FIGURE 19. At left, the two aglet arcs connect to the same interior crossing. At middle, one additional arc is added to this configuration. At right, the unique completion is valid.

bottom aglet crossing to the top interior crossing. Up to symmetry, the diagram is uniquely determined, as shown at right in Figure 20.

Now, suppose that one additional arc connects the top aglet crossing to the top interior crossing. Then one additional arc connects the bottom aglet crossing to the bottom interior crossing. There are two possible configurations, shown at left in Figures 21 and 22. For each configuration, the remaining three arcs must connect aglet crossings to interior crossings. For the first configuration, there is a unique way to make these connections, up to symmetry, shown at right in Figure 21. For the second configuration, there are two possible ways to make these connections, shown at center and left in Figure 22, but one (at right) is disconnected.

Finally, suppose that two additional arcs connect the top aglet crossing to the top interior crossing. Then the single arc connecting the top structure to the bottom structure will force λ to not be reduced. One example is shown in 23. This completes the proof.

□

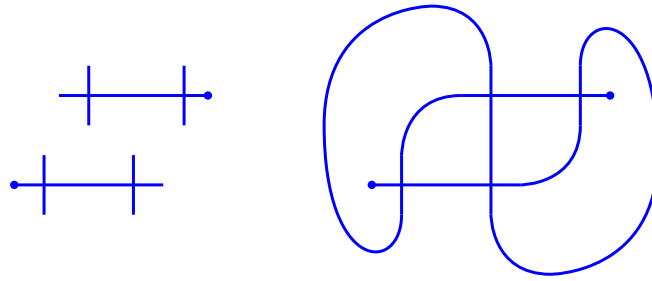


FIGURE 20. At left, the two aglet arcs connect to different interior crossings. At right, the unique completion (up to symmetry) with all arcs connecting the top structure to the bottom structure and no arcs connecting the aglet crossings.

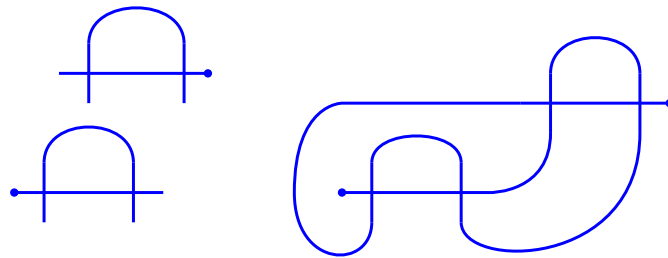


FIGURE 21. At left, one configuration in which one additional arc is attached to the top structure and one is attached to the bottom structure. At right, the unique completion up to symmetry.

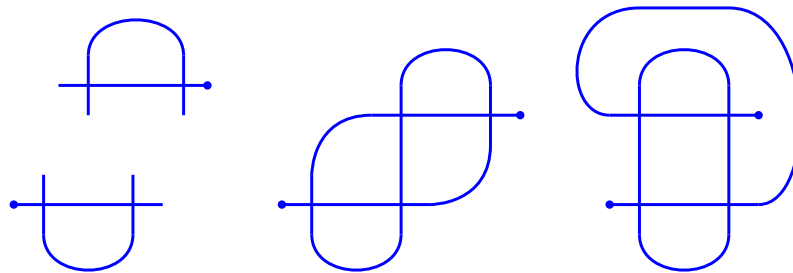


FIGURE 22. At left, another configuration in which one additional arc is attached to the top structure and one is attached to the bottom structure. At center and right, the two possible completions. The completion at right is disconnected.

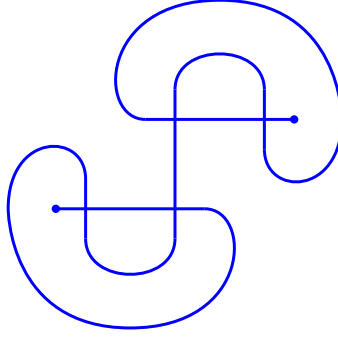


FIGURE 23. If only one arc connects the top structure to the bottom structure, then the diagram λ is not reduced.

4. ALEXANDER POLYNOMIALS AND THE SETS \mathfrak{R}_n^s

In [FMZ24] and [AAC⁺25], the authors used Alexander polynomials to derive new lower bounds for ribbon numbers. In particular, they defined the set

$$\mathfrak{R}_n = \{\Delta_K(t) : r(K) \leq n\}$$

and proved that

Proposition 4.1. *For every n , the set \mathfrak{R}_n is finite and computable.*

In [FMZ24], the authors determined the sets \mathfrak{R}_2 and \mathfrak{R}_3 , where $|\mathfrak{R}_2| = 3$ and $|\mathfrak{R}_3| = 10$. This work was extended in [AAC⁺25], in which the authors computed \mathfrak{R}_4 , where $|\mathfrak{R}_4| = 56$.

Recall the oriented Skein relation for the Alexander and Jones polynomials for oriented links L_+ , L_- , and L_0 that differ within a single crossing:

$$\Delta_{L_+}(t) - \Delta_{L_-}(t) + (t^{-1/2} - t^{1/2})L_0(t) = 0$$

and

$$t^{-1}V_{L_+}(t) - tV_{L_-}(t) + (t^{-1/2} - t^{1/2})V_{L_0}(t) = 0.$$

In what follows, we consistently choose this crossing within a ribbon disk as shown in Figure 24.

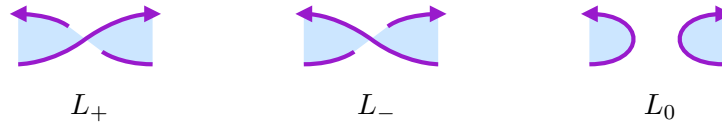


FIGURE 24. Local pictures of changing or resolving a crossing in a ribbon disk used in the proof of Lemma 4.2.

Here, we define an analogously collection of sets of Alexander polynomials for symmetric ribbon knots. However, the structure of symmetric ribbon disks is more rigid, and so we define

$$\mathfrak{R}_n^s = \{\Delta_K(t) : r_s(K) = n \text{ and } K \text{ is prime}\}.$$

It follows immediately from the definition that $\mathfrak{R}_n^s \subset \mathfrak{R}_n$, and so the set \mathfrak{R}_n^s is finite. We will see that this containment is proper for $n = 2, 3, 4$. Note that if $r_s(K) = n$, then K bounds

a symmetric ribbon disk corresponding to a labeled monoid diagram κ with n crossings. In turn κ can be associated with a singular arc diagram. We use the following lemma.

Lemma 4.2. *Suppose K and K' are symmetric ribbon knots bounding disks corresponding to labeled monoid diagrams κ and κ' , respectively, which are identical but with potentially different labelings. If all labelings agree mod 2, then $\Delta_K(t) = \Delta_{K'}(t)$.*

Proof. Consider the Skein relation above and the local pictures of a crossing change performed on a symmetric ribbon disk as shown in Figure 24, where L_+ and L_- are two symmetric ribbon knots corresponding to labeled monoid diagrams with identical labels except for one label differing by two, and L_0 is a two-component ribbon link, where $\Delta_{L_0}(t) = 0$ (see, for instance, [Eis09]). It follows immediately that $\Delta_{L_+}(t) = \Delta_{L_-}(t)$. \square

As a consequence, in order to determine all possible Alexander polynomials for prime knots with symmetric ribbon number n , we need only consider all possible reduced singular arc diagrams with n crossings, along with all possible crossing information and mod 2 labelings. We call such a diagram a *mod 2 labeled knotoid diagram*. Moreover, we can assume that all aglet arcs meet an aglet crossing as an under-crossing (or else we could perform a simplifying aglet move), and so need only consider crossing information for interior crossings. Once we find all possible mod 2 labeled knotoid diagrams, we can use SnapPy [CDGW] within Sage [The21] to compute the corresponding Alexander polynomials. We carry this out for $n = 2, 3, 4$ below.

For $n = 2$, there is only one reduced singular arc diagram with two crossings, 2_1 , shown in Figure 12.

Lemma 4.3. $\mathfrak{A}_2^s = \{1 - 2t + 3t^2 - 2t^3 + t^4, 2 - 5t + 2t^2\}$.

Proof. The reduced singular arc diagram 2_1 gives rise to two possible mod 2 labeled knotoid diagrams, and the corresponding Alexander polynomials are as indicated. \square

For $n = 3$, there are two reduced singular arc diagrams with three crossings, 3_1 and 3_2 , shown in Figure 13. We make our work easier by introducing a new move. A *leaf isotopy* (terminology taken from a similar move in [AAC+25]) on a labeled knotoid diagram is the combination of moves shown in Figure 25.

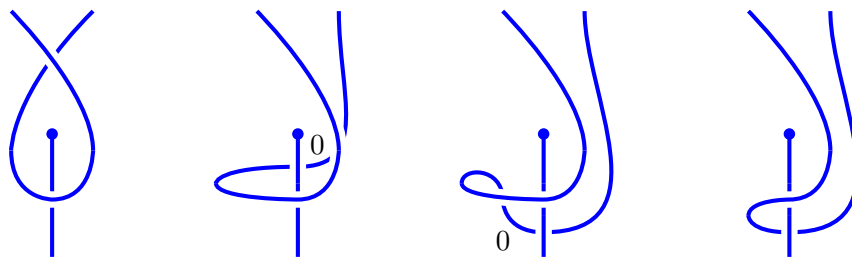


FIGURE 25. A leaf isotopy is a combination of an aglet move, an R3 move, and an R1 move as shown. The only relevant labeling is the zero-labeling of the under-strand in the R3 move occurring between the two middle frames.

Lemma 4.4.

$$\mathfrak{R}_3^s = \{1, 1 - t - t^2 + 3t^3 - t^4 - t^5 + t^6, 1 - 3t^2 + t^4, 1 - 3t + 5t^2 - 7t^3 + 5t^4 - 3t^5 + t^6, 1 - 6t + 11t^2 - 6t^3 + t^4, 2 - 6t + 9t^2 - 6t^3 + 2t^4\}.$$

Proof. Note that 3_2 has a reflection symmetry, and so both choices for the interior crossing will produce identical Alexander polynomials. In addition, one of the choices for the interior crossing of 3_1 can be transformed a leaf isotopy into 3_2 as shown in Figure 26. Thus, we need only consider 3_1 . There are two choices for the interior crossing and two choices for the labels of a mod 2 labeled knotoid diagram associated to 3_1 , yielding eight possibilities. We compute the Alexander polynomials of the corresponding knots, for a total of six distinct polynomials as indicated. \square



FIGURE 26. Converting a labeled knotoid diagram coming from λ_1 to one coming from λ_2 via a leaf isotopy.

Next, we turn to \mathfrak{R}_4^s . Theorem 1.5, stated in Section 1, asserts that the 27 elements of \mathfrak{R}_4^s are given in Table 1. The proof is similar to the proofs of Lemmas 4.3 and 4.4 above, but we relegate its proof to the appendix in Section 8 due to its length.

5. BOUNDS FROM DETERMINANTS

Recall that the determinant $\det(K)$ of a knot K is given by $\det(K) = |\Delta_K(-1)|$. In [FMZ24], the authors proved that for a ribbon knot K ,

$$\det(K) \leq (2^{r(K)} - 1)^2.$$

For low-complexity ribbon knots, this implies

- If $r(K) = 2$, then $\det(K) \leq 9$.
- If $r(K) = 3$, then $\det(K) \leq 49$.
- If $r(K) = 4$, then $\det(K) \leq 225$, and so on.

By evaluating all polynomials in \mathfrak{R}_2^s , \mathfrak{R}_3^s , and \mathfrak{R}_4^s at -1 , we obtain the following immediate corollary of Lemmas 4.3 and 4.4 and Theorem 1.5.

Corollary 5.1. *Suppose K is a prime symmetric ribbon knot.*

- If $r_s(K) = 2$, then $\det(K) = 9$.
- If $r_s(K) = 3$, then $\det(K) = 1$ or 25 .
- If $r_s(K) = 4$, then $\det(K) \leq 49$.

Det	Alexander Polynomial
1	1
1	$1 - 3t^2 + t^4$
1	$1 - t - t^2 + 3t^3 - t^4 - t^5 + t^6$
1	$1 - 2t + t^2 + 2t^3 - 5t^4 + 2t^5 + t^6 - 2t^7 + t^8$
1	$1 - 2t^2 + 3t^4 - 2t^6 + t^8$
1	$1 - 3t - t^2 + 7t^3 - t^4 - 3t^5 + t^6$
1	$1 - 3t + 2t^2 + 3t^3 - 7t^4 + 3t^5 + 2t^6 - 3t^7 + t^8$
1	$2 - 3t - 2t^2 + 7t^3 - 2t^4 - 3t^5 + 2t^6$
1	$2 - 5t^2 + 2t^4$
9	$1 - t - t^3 + 3t^4 - t^5 - t^7 + t^8$
9	$1 - t + t^2 - 3t^3 + t^4 - t^5 + t^6$
9	$1 - t - 3t^2 + 7t^3 - 3t^4 - t^5 + t^6$
9	$1 - 2t + 3t^2 - 2t^3 + t^4$
9	$1 - 2t + 4t^3 - 7t^4 + 4t^5 - 2t^7 + t^8$
9	$2 - 5t + 2t^2$
25	$1 - 2t + 3t^2 - 4t^3 + 5t^4 - 4t^5 + 3t^6 - 2t^7 + t^8$
25	$1 - 3t + 5t^2 - 7t^3 + 5t^4 - 3t^5 + t^6$
25	$1 - 6t + 11t^2 - 6t^3 + t^4$
25	$2 - 6t + 9t^2 - 6t^3 + 2t^4$
25	$6 - 13t + 6t^2$
49	$1 - 3t + 6t^2 - 9t^3 + 11t^4 - 9t^5 + 6t^6 - 3t^7 + t^8$
49	$1 - 4t + 6t^2 - 8t^3 + 11t^4 - 8t^5 + 6t^6 - 4t^7 + t^8$
49	$1 - 5t + 11t^2 - 15t^3 + 11t^4 - 5t^6 + t^6$
49	$2 - 6t + 10t^2 - 13t^3 + 10t^4 - 6t^5 + 2t^6$
49	$2 - 12t + 21t^2 - 12t^3 + 2t^4$
49	$3 - 12t + 19t^2 - 12t^3 + 3t^4$
49	$4 - 12t + 17t^2 - 12t^3 + 4t^4$

TABLE 1. Elements of \mathfrak{R}_4^s , ordered by determinant

In this section, we obtain a similar inequality for knots such that $r_s(K) = 5$. Absent a version of Theorem 1.5 in this case, we take a different approach. Given a knot diagram D , define the *maximal overpass length* $\ell(D)$ to be the largest number of consecutive over-crossings contained in a single strand of D . This quantity is connected to knotoid diagrams via the next lemma. Recall that given a knotoid diagram κ , the *closure* $cl(\kappa)$ is the knot obtained by connecting the aglets with an arc that contains only over-crossings.

Lemma 5.2. *Suppose κ is a knotoid diagram with closure $cl(\kappa)$. Then there is a diagram D for $cl(\kappa)$ such that*

$$c(D) - \ell(D) \leq c(\kappa).$$

Proof. Let D be a diagram for $\text{cl}(\kappa)$ obtained by connecting the aglets of κ with an overpass arc, where D contains n crossings, so that $n = c(D) - c(\kappa)$. It follows that $n \leq \ell(D)$, so that $c(D) - c(\kappa) \leq \ell(D)$. The desired statement follows. \square

In [Kid87], Kidwell connected $c(D) - \ell(D)$ to the degree of the Q -polynomial $Q_K(z)$ of the corresponding knot K , where the Q -polynomial is a specialization $Q_K(z) = F(1, z)$ of the Kauffman polynomial $F_K(a, z)$. Translated to the Kauffman polynomial, Kidwell proved

Theorem 5.3. [Kid87] *Let D be a diagram of a knot K . Then*

$$\deg_z(F_K(a, z)) \leq c(D) - \ell(D).$$

Combining Lemma 5.2 and Theorem 5.3, we have

Corollary 5.4. *Let κ be a knotoid diagram. Then*

$$\deg_z(F_{\text{cl}(\kappa)}(a, z)) \leq c(\kappa).$$

Another useful tool, also proved by Kidwell as an appendix in [Sto03], is

Theorem 5.5. [Sto03, Theorem 2.1] *Suppose κ is a knotoid diagram. Then there is a diagram D for $\text{cl}(\kappa)$ such that*

$$c(D) \leq \frac{3}{2} \cdot c(\kappa).$$

A knot diagram D is called *prime* if there does not exist a simple closed curve c meeting D in two points such that there are crossings of D on both sides of c . The *breadth* $\text{breadth}(V_K(t))$ of the Jones polynomial $V_K(t)$ is the difference between the largest and smallest degrees appearing in $V_K(t)$. Murasugi and Thistlethwaite proved that if D is a prime, non-alternating diagram for a knot K , then $c(D) > \text{breadth}(V_K(t))$ [Mur87, Thi87].

We require one more technical, highly specialized lemma.

Lemma 5.6. *Suppose κ is a knotoid diagram such that $\text{cl}(\kappa)$ is the connected sum of the trefoil and figure eight knot. Then either κ is not prime, or $c(\kappa) > 5$.*

Proof. Suppose κ is a knotoid diagram such that $\text{cl}(\kappa) = K_1 \# K_2$, where K_1 is the trefoil and K_2 is the figure eight knot, and let $J = \text{cl}(\kappa)$. Using the Kauffman polynomial data from the KnotInfo database [LM26] along with the fact that the Kauffmann polynomial is multiplicative under connected sum, we have that $\deg_z(F_J(a, z)) = 5$, so that $c(\kappa) \geq 5$ by Corollary 5.4. Suppose $c(\kappa) = 5$, and note that κ cannot admit a simplifying R1 move. By Theorem 5.5, there is a diagram D for J such that $c(D) \leq 7$, and since $c(J) = 7$, we must have $c(D) = 7$. Let α denote the arc used to obtain D from κ , so that α contains two over-crossings, implying that D is non-alternating. By Murasugi and Thistlethwaite's Theorem along with the fact that $\text{breadth}(V_J(t)) = 7$, it follows that D is not prime, so there exists a curve c meeting D in two points, with crossings on either side of c .

It follows that we can express D as $D_1 \# D_2$, and since D is a minimal-crossing diagram, we may assume without loss of generality that D_1 is a 3-crossing diagram for K_1 and D_2 is a 4-crossing diagram for K_2 . If the arc α meets c in two points, then the knotoid diagram κ is not connected, a contradiction. If α meets c in one point, then the knotoid diagram κ also meets c in one point. As $c(D_1) = 3$, $c(D_2) = 4$, and α contains two crossings, it follows that κ contains crossings on either side of c , so that κ is not prime (since κ cannot admit a simplifying R1 move). Finally, if α is disjoint from c , then α is contained entirely within D_1 or D_2 .

If α is contained entirely within D_1 , then so are both aglets of κ . By cutting κ open along c and gluing in an arc of c , we can obtain a knotoid κ' such that $c(\kappa') = 1$ and $\text{cl}(\kappa') = K_1$, contradicting Corollary 5.4. See Figure 27. On the other hand, if α is contained entirely within D_2 , cutting κ open along c and gluing in an arc of c yields a knotoid κ'' such that $c(\kappa'') = 2$ and $\text{cl}(\kappa'') = K_2$, another contradiction to Corollary 5.4. We conclude that either $c(\kappa) > 5$ or κ is not prime. \square

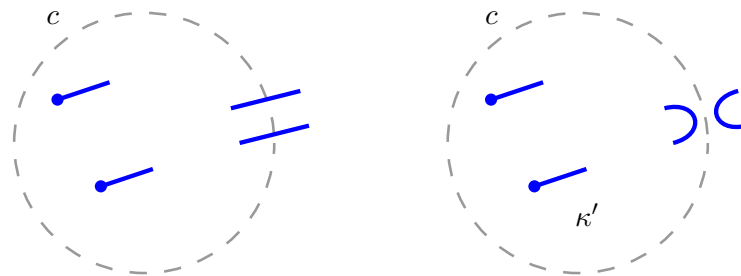


FIGURE 27. If both aglets of κ are inside of D_1 , we surger κ along c to obtain a knotoid κ' within D_1 .

We have assembled all of the necessary ingredients to prove our next bound on symmetric ribbon number, Theorem 1.6, which asserts that if $r_s(K) = 5$, then $\det(K) \leq 169$.

Proof of Theorem 1.6. Suppose $r_s(K) = 5$. Then K bounds a symmetric ribbon disk with associated labeled knotoid diagram κ such that $c(\kappa) = 5$. Let $J = \text{cl}(\kappa)$. By Corollary 5.4 and Theorem 5.5, we have

$$\deg_z(F_J(a, z)) \leq 5 \text{ and } c(J) \leq 7.$$

If J is prime, then using the Kauffman polynomial and determinant data from the KnotInfo database [LM26], we see that J must satisfy $c(J) \leq 6$, since all 7-crossing knots have Kauffman polynomials with z -degree six. The maximum possible determinant of such J is 13, so we have $\det(J) \leq 13$, and by Lemma 2.4, it follows that $\det(K) \leq 169$.

On the other hand, suppose J is composite. Since crossing number is additive under connected sum for alternating knots, it follows that $J = J_1 \# J_2$, where $c(J_1) \leq 3$ and $c(J_2) \leq 4$. If both J_1 and J_2 are trefoils, then $\det(K) \leq 81$. Otherwise, J_1 is the trefoil and J_2 is the figure eight knot. By Lemma 5.6 and the assumption that $c(\kappa) = 5$, we have that κ is not prime. But this implies K is not prime, a contradiction. \square

Remark 5.7. The proof of Lemma 5.6 can be adapted to knots summands with greater crossing numbers, so that similar bounds can be obtained for larger symmetric ribbon numbers. Using the KnotInfo data up to 12 crossings, we can generalize the above to obtain the following:

- If K is a prime symmetric ribbon knot such that $r_s(K) = 6$, then $\det(K) \leq 21^2$.
- If K is a prime symmetric ribbon knot such that $r_s(K) = 7$, then $\det(K) \leq 75^2$.
- If K is a prime symmetric ribbon knot such that $r_s(K) = 8$, then $\det(K) \leq 121^2$.

We do not, however, use these results in our tabulation below. Consider the sequence $\{3, 5, 7, 13, 21, 75, 121, \dots\}$. Squares of its entries show up as upper bounds in Corollary 5.1, Theorem 1.6, and the inequalities above. This sequence coincides with the maximal determinant of a knot with n crossings, starting with $n = 3$ [Sto03]. In general, we conjecture

that the maximum determinant of a prime symmetric ribbon knot K with $r_s(K) = n$ is the square of the maximum determinant of a prime knot J with $c(J) = n + 1$.

6. JONES POLYNOMIALS AND SYMMETRIC RIBBON KNOTS

In this section, we determine all possible Jones polynomials for symmetric ribbon knots K with $r_s(K) = 2$ or $r_s(K) = 3$ and $\det(K) = 25$. Although these families are not finite, as in the case of \mathfrak{R}_n^s , they are manageable enough to extract additional lower bounds on symmetric ribbon numbers. Recall the oriented skein relation for the Jones polynomial from Section 4. We will let U_2 denote the two-component unlink, noting that $V_{U_2}(t) = -t^{-1/2} - t^{1/2}$. Computations are performed using SnapPy [CDGW] inside of Sage [The21]. Observe that SnapPy within Sage uses the variable q for the Jones polynomial, and we convert to the variable t via the usual substitution $t = q^2$ (conversely, $q = -t^{1/2}$).

Proposition 6.1. *Suppose K is a knot with $r_s(K) = 2$. There is a family $\{K_n\}$ of symmetric ribbon knots such that $K \in \{K_n\}$ and*

$$V_{K_n}(t) = (-t)^n(-t^{-3} + t^{-2} - t^{-1} + 2 - t + t^2 - t^3) + 1.$$

Proof. By Lemma 3.1, if K satisfies $r_s(K) = 2$, then K bounds a symmetric ribbon disk corresponding to the labeled knotoid diagram κ_n in Figure 28. Let K_n denote the knot arising from the label n .

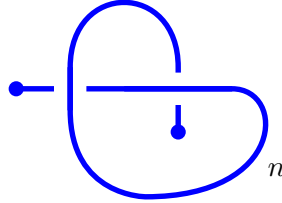


FIGURE 28. The only labeled knotoid diagram κ_n for knots K with $r_s(K) = 2$.

There are two cases to consider, whether n positive or negative. The proof proceeds by induction, and we verify the base cases for K_0 and K_1 by direction computation. First, let $n > 1$ and suppose the proposition holds for K_{n-2} . Choosing L_+ , L_- , and L_0 as in Figure 24, we have that $L_+ = K_n$, $L_- = K_{n-2}$, and $L_0 = U_2$. Let $f(t) = -t^{-3} + t^{-2} - t^{-1} + 2 - t + t^2 - t^3$. Applying the skein relation, we have

$$\begin{aligned} V_{K_n}(t) &= t^2 V_{K_{n-2}}(t) - (t^{1/2} - t^{3/2})V_{U_2}(t) \\ &= t^2((-t)^{n-2} \cdot f(t) + 1) - (t^{1/2} - t^{3/2})(-t^{-1/2} - t^{1/2}) \\ &= (-t)^n \cdot f(t) + t^2 - t^2 + 1 \\ &= (-t)^n \cdot f(t) + 1. \end{aligned}$$

On the other hand, if $n < 0$, we suppose that the proposition holds for K_{n+2} and apply the skein relation with $K_n = L_-$, $K_{n+2} = L_+$, and $L_0 = U_2$. We have

$$\begin{aligned} V_{K_n}(t) &= t^{-2} V_{K_{n+2}}(t) + (t^{-3/2} - t^{-1/2})V_{U_2}(t) \\ &= t^{-2}((-t)^{n+2} \cdot f(t) + 1) + (t^{-3/2} - t^{-1/2})(-t^{-1/2} - t^{1/2}) \\ &= (-t)^n \cdot f(t) + t^{-2} - t^{-2} + 1 \\ &= (-t)^n \cdot f(t) + 1. \end{aligned}$$

□

Turning to the case $r_s(K) = 3$, recall from Lemmas 3.2 and 4.4 that there are two possible labeled knotoid diagrams $\kappa_{m,n}$ and $\kappa'_{m,n}$ corresponding to K . These diagrams are shown in Figure 29.

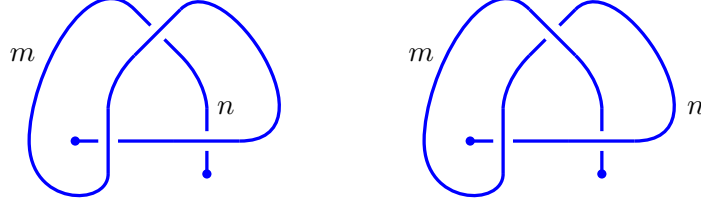


FIGURE 29. The only two labeled knotoid diagrams $\kappa_{m,n}$ (left) and $\kappa'_{m,n}$ (right) associated to knots K with $r_s(K) = 3$.

Proposition 6.2. *Suppose K is a knot with $r_s(K) = 3$ and $\det(K) = 25$. There is a family $\{K_{m,n}\}$ of symmetric ribbon knots such that $K \in \{K_{m,n}\}$ and*

$$V_{K_{m,n}}(t) = (-t)^{m+n}(t^{-4} - 2t^{-3} + 3t^{-2} - 4t^{-1} + 4 - 4t + 3t^2 - 2t^3 + t^4) + 1.$$

Proof. Suppose $r_s(K) = 3$ and $\det(K) = 25$. Note that $\text{cl}(\kappa_{m,n})$ is the unknot, and so by Lemma 2.4 and the assumption that $\det(K) = 25$, we have that K must correspond to the other family of diagrams, $\kappa'_{m,n}$ (the closure of which is the figure eight knot). It follows that $K = K_{m,n}$, the knot arising from $\kappa'_{m,n}$, for some integers m and n . First, we note that performing an oriented smoothing in the twist region labeled m yields U_2 , as does performing an oriented smoothing in the twist region labeled n . Thus, for any m , we can choose $L_+ = K_{m+2,n}$, $L_- = K_{m,n}$, and $L_0 = U_2$ to satisfy the oriented skein relation. However, we can alternatively choose $L_+ = K_{m,n+2}$, $L_- = K_{m,n}$, and $L_0 = U_2$. It follows that $V_{L_{m+2,n}}(t) = V_{L_{m,n+2}}(t)$. A similar argument shows that $V_{L_{m-2,n}}(t) = V_{L_{m,n-2}}(t)$. As a consequence, we need only show that the desired statement holds for knots of the form $K_{0,n}$ and $K_{1,n}$.

As above, we proceed by induction on m , verifying the formula for $K_{0,0}$, $K_{0,1}$, $K_{1,0}$, and $K_{1,1}$ by direct computation. Suppose $n > 1$ and suppose the formula holds for $K_{i,n-2}$, with $i = 0$ or 1 . Let $L_+ = K_{i,n}$, $L_- = K_{i,n-2}$, and $L_0 = U_2$, and let $f(t) = t^{-4} - 2t^{-3} + 3t^{-2} - 4t^{-1} + 4 - 4t + 3t^2 - 2t^3 + t^4$. Applying the skein relation yields

$$\begin{aligned} V_{K_{i,n}}(t) &= t^2 V_{K_{i,n-2}}(t) - (t^{1/2} - t^{3/2})V_{U_2}(t) \\ &= t^2((-t)^{i+n-2} \cdot f(t) + 1) - (t^{1/2} - t^{3/2})(-t^{-1/2} - t^{1/2}) \\ &= (-t)^{i+n} \cdot f(t) + t^2 - t^2 + 1 \\ &= (-t)^{i+n} \cdot f(t) + 1. \end{aligned}$$

Similarly, if $n < 0$, let $L_+ = K_{i,n}$, $L_- = K_{i,n+2}$, and $L_0 = U_2$. Then

$$\begin{aligned} V_{K_{i,n}}(t) &= t^{-2} V_{K_{i,n+2}}(t) + (t^{-3/2} - t^{-1/2})V_{U_2}(t) \\ &= t^{-2}((-t)^{i+n+2} \cdot f(t) + 1) + (t^{-3/2} - t^{-1/2})(-t^{-1/2} - t^{1/2}) \\ &= (-t)^{i+n} \cdot f(t) + t^{-2} - t^{-2} + 1 \\ &= (-t)^{i+n} \cdot f(t) + 1. \end{aligned}$$

□

As a corollary, we show

Corollary 6.3. *The knots $K \in \{11n_{39}, 12n_{256}, 12n_{257}, 12n_{394}, 12n_{870}\}$ satisfy $r_s(K) \geq 4$.*

Proof. From KnotInfo, $\det(K) = 25$, implying that $r_s(K) \geq 3$ by Corollary 5.1. If $r_s(K) = 3$, then by Proposition 6.2, all coefficients c_i of $V_K(t)$ satisfy $|c_i| \leq 5$, and at most one satisfies $|c_i| = 5$. However, from KnotInfo,

$$\begin{aligned} V_{11n_{39}}(t) &= -t^{-4} + t^{-3} - t^{-1} + 4 - 4t + 5t^2 - 5t^3 + 4t^4 - 3t^5 + t^6 \\ V_{12n_{256}}(t) &= -t^{-4} + 2t^{-3} - 2t^{-2} + t^{-1} + 2 - 3t + 5t^2 - 6t^3 + 6t^4 - 5t^5 + 3t^6 - t^7 \\ V_{12n_{257}}(t) &= t^{-6} - 3t^{-5} + 4t^{-4} - 5t^{-3} + 5t^{-2} - 4t^{-1} + 4 - t + t^3 - t^4 \\ V_{12n_{394}}(t) &= t^{-5} - t^{-4} + t^{-2} - 3t^{-1} + 5 - 5t + 5t^2 - 4t^3 + 3t^4 - t^5 \\ V_{12n_{870}}(t) &= -t^{-3} - t^{-2} + 2 - 3t + 4t^2 - 5t^3 + 5t^4 - 4t^5 + 3t^6 - t^7. \end{aligned}$$

Hence, $r_s(K) \geq 4$. □

Remark 6.4. Proposition 6.2 not only provides a new obstruction to $r_s(K) = 3$; it also helps us search for previously unknown symmetric ribbon disks. Consider the symmetric ribbon knots $11n_{37}$ and $12n_{414}$, both of which have determinant 25. Applying Prop 2.6 to the symmetric union presentations for these knots in [Lam21a] yields $r_s(11n_{37}) \leq 4$ and $r_s(12n_{414}) \leq 4$. Using KnotInfo, we have

$$\begin{aligned} V_{11n_{37}}(t) &= t^{-6} - 2t^{-5} + 3t^{-4} - 4t^{-3} + 4t^{-2} - 4t^{-1} + 4 - 2t + t^2 \\ V_{12n_{414}}(t) &= -t^{-7} + 2t^{-6} - 3t^{-5} + 4t^{-4} - 4t^{-3} + 4t^{-2} - 3t^{-1} + 3 - t. \end{aligned}$$

Thus, by Proposition 6.2, if $r_s(11n_{37}) = 3$, then $11n_{37} = K_{m,n}$, where $m+n = -2$. Similarly, if $r_s(12n_{414}) = 3$, then $12n_{414} = K_{m,n}$ with $m+n = -3$. After searching through low-complexity possibilities, we verified with SnapPy that indeed $11n_{37} = K_{-3,1}$ and $12n_{414} = K_{-4,1}$, shown in Figure 3. Note further that Lamm’s symmetric union presentations for $11n_{37}$ and $12n_{414}$ are marked “m” for minimal in Table 1 of [Lam21a]. This notion of minimality does not refer to symmetric ribbon number but rather to the crossing number of the symmetric union presentation. Lamm’s symmetric union presentation for $11n_{37}$ has symmetric ribbon number four with crossing number 11, while ours has symmetric ribbon number three and crossing number 12. Similarly, Lamm’s symmetric union presentation for $12n_{414}$ has symmetric ribbon number four with crossing number 12, while ours has symmetric ribbon number three and crossing number 13. Finally, the partial knot for Lamm’s presentations is 5_1 , while the partial knot for our presentations is 4_1 .

7. TABULATION OF SYMMETRIC RIBBON NUMBERS

In this section, we put our tools to work, tabulating the symmetric ribbon numbers for symmetric ribbon knots up to 12 crossings. As noted in the statement of Theorem 1.2, symmetric ribbon numbers for

- prime symmetric ribbon knots with 11 or fewer crossings appear in Table 2,
- prime nonalternating symmetric ribbon knots with 12 crossings appear in Table 3, and
- prime alternating symmetric ribbon knots with 12 crossings appear in Table 4.

In addition, lower bounds for the symmetric ribbon numbers of the 15 knots with 12 or fewer crossings that are not known to be symmetric are included in Table 5.

For reference, each table row includes the knot determinant, Alexander polynomial, the lower bound for the ribbon number taken from [FMZ24] (for knots with 11 or fewer crossings) or [AAC⁺25] (for knots with 12 crossings), the symmetric ribbon number (or a range

of possible symmetric ribbon numbers), and the justification for the lower bound on the symmetric ribbon number. Upper bounds for symmetric ribbon numbers are computed using Proposition 2.6 along with the symmetric union presentations from [Lam00] (for knots with 10 or fewer crossings) or [Lam21a] (for knots with 11 or 12 crossings). The only exceptions are the upper bounds for 10_{87} , which comes from the diagram in [EL07], and the knots $11n_{37}$ and $12n_{414}$, noted in Remark 6.4 and Figure 3.

8. APPENDIX: PROOF OF THEOREM 1.5

We first note some overlap in the eight reduced singular arc diagrams $4_1, \dots, 4_8$, which can be eliminated via leaf isotopies. Figures 30, 31, and 32 include singular arc diagrams with crossing information added at only one relevant double point, since the leaf isotopy can differ based on this crossing information. In Figure 30, we see that two possible leaf isotopies convert a diagram of type 4_1^a to type 4_7 or type 4_1^b to type 4_8 . Similarly, in Figure 31, the two possible leaf isotopies convert a labeled knotoid diagram of type 4_5^a to type 4_4 or type 4_5^b to type 4_7 . Finally, in Figure 32, two possible leaf isotopies convert a labeled knotoid diagram of type 4_6^a to type 4_5 or type 4_6^b to type 4_1 . Therefore, after simplifying with leaf isotopies, we need only consider labeled knotoid diagrams of types $4_2, 4_3, 4_4, 4_7$, and 4_8 .

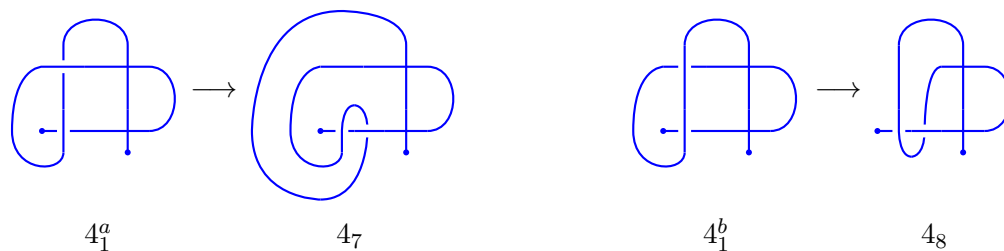


FIGURE 30. Two possible leaf isotopies on a labeled knotoid diagram of type 4_1 .

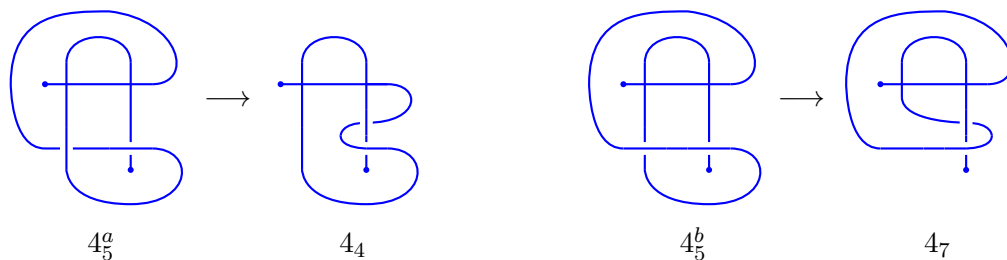


FIGURE 31. Two possible leaf isotopies on a labeled knotoid diagram of type 4_5 . In the second frame, an arc of the diagram 4_4 has been redrawn via planar isotopy in S^2 .

Proof of Theorem 1.5. In order to find all possible Alexander polynomials of knots K with $r_s(K) = 4$, it suffices to compute Alexander polynomials for all mod 2 labeled knotoid diagrams of types $4_2, 4_3, 4_4, 4_7$, and 4_8 . Each type involves two choices for each interior crossing and two choices for each of three strands, for a total of 32 possibilities. Below, we list all distinct Alexander polynomials associated to each type.

K	$\det(K)$	$\Delta_K(t)$	$r(K) \geq$	$r_s(K)$	lower
6_1	9	$2 - 5t + 2t^2$	2	2	Lem. 2.2
8_8	25	$2 - 6t + 9t^2 - 6t^3 + 2$	3	3	Lem. 2.2
8_9	25	$1 - 3t + 5t^2 - 7t^3 + 5t^4 - 3t^3 + t^6$	3	3	Lem. 2.2
8_{20}	9	$1 - 2t + 3t^2 - 2t^3 + t^4$	2	2	Lem. 2.2
9_{27}	49	$1 - 5t + 11t^2 - 15t^3 + 11t^4 - 5t^5 + t^6$	3	4	Lem. 4.4
9_{41}	49	$3 - 12t + 19t^2 - 12t^3 + 3t^4$	3	4	Lem. 4.4
9_{46}	9	$2 - 5t + 2t^2$	2	2	Lem. 2.2
10_3	25	$6 - 13t + 6t^2$	4	4	Lem. 2.2
10_{22}	49	$2 - 6t + 10t^2 - 13t^3 + 10t^4 - 6t^5 + 2t^6$	4	4	Lem. 2.2
10_{35}	49	$2 - 12t + 21t^2 - 12t^3 + 2t^4$	4	4	Lem. 2.2
10_{42}	81	$1 - 7t + 19t^2 - 27t^3 + 19t^4 - 7t^5 + t^6$	4	5	Thm. 1.5
10_{48}	49	$1 - 3t + 6t^2 - 9t^3 + 11t^4 - 9t^5 + 6t^6 - 3t^7 + t^8$	4	4	Lem. 2.2
10_{75}	81	$1 - 7t + 19t^2 - 27t^3 + 19t^4 - 7t^5 + t^6$	4	5	Thm. 1.5
10_{87}	81	$2 - 9t + 18t^2 - 23t^3 + 18t^4 - 9t^5 + 2t^6$	4	5	Thm. 1.5
10_{99}	81	$1 - 4t + 10t^2 - 16t^3 + 19t^4 - 16t^5 + 10t^6 - 4t^7 + t^8$	4	5	Thm. 1.5
10_{123}	121	$1 - 6t + 15t^2 - 24t^3 + 29t^4 - 24t^5 + 15t^6 - 6t^7 + t^8$	4	5	Lem. 2.2
10_{129}	25	$2 - 6t + 9t^2 - 6t^3 + 2$	3	3	Lem. 2.2
10_{137}	25	$1 - 6t + 11t^2 - 6t^3 + t^4$	3	3	Lem. 2.2
10_{140}	9	$1 - 2t + 3t^2 - 2t^3 + t^4$	2	2	Lem. 2.2
10_{153}	1	$1 - t + t^2 - 3t^3 + t^4 - t^5 + t^6$	3	3	Lem. 2.2
10_{155}	25	$1 - 3t + 5t^2 - 7t^3 + 5t^4 - 3t^3 + t^6$	3	3	Lem. 2.2
$11a_{28}$	121	$1 - 6t + 15t^2 - 24t^3 + 29t^4 - 24t^5 + 15t^6 - 6t^7 + t^8$	4	5	Thm. 1.5
$11a_{35}$	121	$1 - 5t + 14t^2 - 25t^3 + 31t^4 - 25t^5 + 14t^6 - 5t^7 + t^8$	4	5	Thm. 1.5
$11a_{36}$	121	$2 - 12t + 28t^2 - 37t^3 + 28t^4 - 12t^5 + t^6$	4	5	Thm. 1.5
$11a_{58}$	81	$2 - 9t + 18t^2 - 23t^3 + 18t^4 - 9t^5 + 2t^6$	4	5, 6, 7, 8	Thm. 1.5
$11a_{87}$	121	$2 - 11t + 28t^2 - 39t^3 + 28t^4 - 11t^5 + 2t^6$	4	5	Thm. 1.5
$11a_{96}$	121	$1 - 9t + 29t^2 - 43t^3 + 29t^4 - 9t^5 + t^6$	4	5	Thm. 1.5
$11a_{115}$	121	$3 - 13t + 27t^2 - 35t^3 + 27t^4 - 13t^5 + 3t^6$	4	5	Thm. 1.5
$11a_{164}$	169	$1 - 7t + 20t^2 - 35t^3 + 43t^4 - 35t^5 + 20t^6 - 7t^7 + t^8$	4	5, 6	Thm. 1.5
$11a_{169}$	121	$2 - 12t + 28t^2 - 37t^3 + 28t^4 - 12t^5 + t^6$	4	5	Thm. 1.5
$11a_{316}$	121	$1 - 5t + 14t^2 - 25t^3 + 31t^4 - 25t^5 + 14t^6 - 5t^7 + t^8$	4	5	Thm. 1.5
$11a_{326}$	169	$1 - 6t + 19t^2 - 36t^3 + 45t^4 - 36t^5 + 19t^6 - 6t^7 + t^8$	4	5, 6	Thm. 1.5
$11n_4$	49	$1 - 5t + 11t^2 - 15t^3 + 11t^4 - 5t^5 + t^6$	3	4	Lem. 4.4
$11n_{21}$	49	$1 - 5t + 11t^2 - 15t^3 + 11t^4 - 5t^5 + t^6$	3	4	Lem. 4.4
$11n_{37}$	25	$1 - 3t + 5t^2 - 7t^3 + 5t^4 - 3t^3 + t^6$	3	3	Lem. 2.2
$11n_{39}$	25	$2 - 6t + 9t^2 - 6t^3 + 2$	3	4	Cor. 6.3
$11n_{42}$	1	1	3	3	Lem. 2.2
$11n_{49}$	1	$1 - 3t^2 + t^4$	3	3	Lem. 2.2
$11n_{50}$	25	$2 - 6t + 9t^2 - 6t^3 + 2$	3	3	Lem. 2.2
$11n_{83}$	49	$3 - 12t + 19t^2 - 12t^3 + 3t^4$	3	4	Lem 4.4
$11n_{116}$	1	$1 - 3t^2 + t^4$	3	3	Lem 4.4
$11n_{132}$	25	$2 - 6t + 9t^2 - 6t^3 + 2$	3	3	Lem 4.4
$11n_{139}$	9	$2 - 5t + 2t^2$	2	2	Lem 4.4
$11n_{172}$	49	$1 - 5t + 11t^2 - 15t^3 + 11t^4 - 5t^5 + t^6$	3	4	Lem 4.4

TABLE 2. Symmetric ribbon number data and justifications for prime symmetric ribbon knots up to 11 crossings

$$\begin{aligned}
 4_2 : & \quad 1 \\
 & \quad 1 - 3t^2 + t^4 \\
 & \quad 1 - t - t^2 + 3t^3 - t^4 - t^5 + t^6 \\
 & \quad 1 - 3t - t^2 + 7t^3 - t^4 - 3t^5 + t^6 \\
 & \quad 1 - 3t + 2t^2 + 3t^3 - 7t^4 + 3t^5 + 2t^6 - 3t^7 + t^8
 \end{aligned}$$

K	$\det(K)$	$\Delta_K(t)$	$r(K) \geq$	$r_s(K)$	lower
12n ₄	81	$1 - 7t + 19t^2 - 27t^3 + 19t^4 - 7t^5 + t^6$	4	5	Thm. 1.5
12n ₁₉	1	$1 - 3t - t^2 + 7t^3 - t^4 - 3t^5 + t^6$	4	4	Lem. 2.2
12n ₂₃	9	$2 - 5t + 2t^2$	3	4, 5	Lem. 4.4
12n ₂₄	49	$1 - 5t + 11t^2 - 15t^3 + 11t^4 - 5t^5 + t^6$	3	4	Lem. 4.4
12n ₄₃	81	$1 - 5t + 10t^2 - 15t^3 + 19t^4 - 15t^5 + 10t^6 - 5t^7 + t^8$	4	5	Thm. 1.5
12n ₄₈	49	$2 - 12t + 21t^2 - 12t^3 + 2t^4$	4	4	Lem 2.2
12n ₄₉	81	$4 - 20t + 33t^2 - 20t^3 + 4t^4$	4	5, 6, 7, 8	Thm. 1.5
12n ₈₇	49	$4 - 12t + 17t^2 - 12t^3 + 4t^4$	4	4	Lem. 2.2
12n ₁₀₆	81	$1 - 4t + 10t^2 - 16t^3 + 19t^4 - 16t^5 + 10t^6 - 4t^7 + t^8$	4	5	Thm. 1.5
12n ₁₄₅	25	$1 - 6t + 11t^2 - 6t^3 + t^4$	3	3	Lem. 2.2
12n ₁₇₀	81	$6 - 20t + 29t^2 - 20t^3 + 6t^4$	4	5	Thm. 1.5
12n ₂₁₄	1	$1 - t - t^2 + 3t^3 - t^4 - t^5 + t^6$	3	3	Lem. 2.2
12n ₂₅₆	25	$2 - 6t + 9t^2 - 6t^3 + 2t^4$	3	4	Cor. 6.3
12n ₂₅₇	25	$2 - 6t + 9t^2 - 6t^3 + 2t^4$	3	4	Cor. 6.3
12n ₂₆₈	9	$2 - 5t + 2t^2$	3	4	Lem. 4.4
12n ₂₇₉	25	$1 - 6t + 11t^2 - 6t^3 + t^4$	3	3	Lem. 2.2
12n ₂₈₈	49	$4 - 12t + 17t^2 - 12t^3 + 4t^4$	4	4	Lem. 2.2
12n ₃₀₉	1	$1 - t - t^2 + 3t^3 - t^4 - t^5 + t^6$	3	3	Lem. 2.2
12n ₃₁₂	49	$1 - 5t + 11t^2 - 15t^3 + 11t^4 - 5t^5 + t^6$	3	4	Lem 4.4
12n ₃₁₃	1	1	3	3	Lem. 2.2
12n ₃₁₈	1	$1 - t - t^2 + 3t^3 - t^4 - t^5 + t^6$	3	3	Lem. 2.2
12n ₃₆₀	49	$3 - 12t + 19t^2 - 12t^3 + 3t^4$	3	4	Lem 4.4
12n ₃₈₀	81	$2 - 9t + 18t^2 - 23t^3 + 18t^4 - 9t^5 + 2t^6$	4	5	Thm. 1.5
12n ₃₉₃	49	$3 - 12t + 19t^2 - 12t^3 + 3t^4$	3	4	Lem. 4.4
12n ₃₉₄	25	$1 - 6t + 11t^2 - 6t^3 + t^4$	3	4	Cor. 6.3
12n ₃₉₇	49	$1 - 5t + 11t^2 - 15t^3 + 11t^4 - 5t^5 + t^6$	3	4	Lem. 4.4
12n ₃₉₉	81	$1 - 7t + 19t^2 - 27t^3 + 19t^4 - 7t^5 + t^6$	4	5	Thm. 1.5
12n ₄₁₄	25	$2 - 6t + 9t^2 - 6t^3 + 2t^4$	3	3	Lem. 2.2
12n ₄₂₀	81	$1 - 7t + 19t^2 - 27t^3 + 19t^4 - 7t^5 + t^6$	4	5	Thm. 1.5
12n ₄₃₀	1	1	3	3	Lem. 2.2
12n ₄₄₀	81	$2 - 9t + 18t^2 - 23t^3 + 18t^4 - 9t^5 + 2t^6$	4	5	Thm. 1.5
12n ₄₆₂	25	$1 - 6t + 11t^2 - 6t^3 + t^4$	3	3	Lem. 2.2
12n ₅₀₁	49	$4 - 12t + 17t^2 - 12t^3 + 4t^4$	3	4	Lem. 4.4
12n ₅₀₄	121	$1 - 6t + 15t^2 - 24t^3 + 29t^4 - 24t^5 + 15t^6 - 6t^7 + t^8$	4	5, 6	Thm. 1.5
12n ₅₅₃	81	$4 - 20t + 33t^2 - 20t^3 + 4t^4$	4	5	Thm. 1.5
12n ₅₅₆	81	$4 - 20t + 33t^2 - 20t^3 + 4t^4$	4	5	Thm. 1.5
12n ₅₈₂	9	$1 - 2t + 3t^2 - 2t^3 + t^4$	2	2	Lem. 2.2
12n ₆₀₅	9	$1 - 2t + 4t^3 - 7t^4 + 4t^5 - 2t^7 + t^8$	4	4	Lem. 2.2
12n ₆₃₆	81	$1 - 7t + 19t^2 - 27t^3 + 19t^4 - 7t^5 + t^6$	4	5	Thm. 1.5
12n ₆₅₇	81	$1 - 4t + 9t^2 - 16t^3 + 21t^4 - 16t^5 + 9t^6 - 4t^7 + t^8$	4	5	Thm 1.5
12n ₆₇₀	25	$1 - 2t + 3t^2 - 4t^3 + 5t^4 - 4t^5 + 3t^6 - 2t^7 + t^8$	4	4	Lem. 2.2
12n ₆₇₆	9	$2 - 2t - 4t^2 + 9t^3 - 4t^4 - 2t^5 + 2t^6$	4	5	Thm. 1.5
12n ₇₀₂	121	$2 - 12t + 28t^2 - 37t^3 + 28t^4 - 12t^5 + 2t^6$	4	5	Thm. 1.5
12n ₇₀₆	49	$1 - 4t + 6t^2 - 8t^3 + 11t^4 - 8t^5 + 6t^6 - 4t^7 + t^8$	4	4, 5, 6	Lem. 2.2
12n ₇₀₈	49	$1 - 3t + 6t^2 - 9t^3 + 11t^4 - 9t^5 + 6t^6 - 3t^7 + t^8$	4	4	Lem. 2.2
12n ₇₂₁	25	$1 - 2t + 3t^2 - 4t^3 + 5t^4 - 4t^5 + 3t^6 - 2t^7 + t^8$	4	4	Lem. 2.2
12n ₇₆₈	25	$1 - 3t + 5t^2 - 7t^3 + 5t^4 - 3t^5 + t^6$	3	3	Lem. 2.2
12n ₇₈₂	81	$2 - 8t + 18t^2 - 25t^3 + 18t^4 - 8t^5 + 2t^6$	4	5	Thm. 1.5
12n ₈₀₂	121	$1 - 5t + 14t^2 - 25t^3 + 31t^4 - 25t^5 + 14t^6 - 5t^7 + t^8$	4	5	Thm. 1.5
12n ₈₁₇	49	$2 - 6t + 10t^2 - 13t^3 + 10t^4 - 6t^5 + 2t^6$	4	4	Lem. 2.2
12n ₈₃₈	25	$1 - 6t + 11t^2 - 6t^3 + t^4$	3	3	Lem. 2.2
12n ₈₇₀	25	$1 - 3t + 5t^2 - 7t^3 + 5t^4 - 3t^5 + t^6$	3	4	Cor. 6.3
12n ₈₇₆	81	$2 - 8t + 18t^2 - 25t^3 + 18t^4 - 8t^5 + 2t^6$	4	5	Thm. 1.5

TABLE 3. Symmetric ribbon number data and justifications for prime non-alternating symmetric ribbon knots with 12 crossings

K	$\det(K)$	$\Delta_K(t)$	$r(K) \geq$	$r_s(K)$	lower
12a ₃	169	$2 - 14t + 40t^2 - 57t^3 + 40t^4 - 14t^5 + 2t^6$	4	5, 6	Thm. 1.5
12a ₅₄	169	$3 - 17t + 39t^2 - 51t^3 + 39t^4 - 17t^5 + 3t^6$	4	5	Thm. 1.5
12a ₇₇	225	$1 - 7t + 24t^2 - 49t^3 + 63t^4 - 49t^5 + 24t^6 - 7t^7 + t^8$	4	6, 7, 8	Thm. 1.6
12a ₁₀₀	225	$3 - 21t + 53t^2 - 71t^3 + 53t^4 - 21t^5 + 3t^6$	4	6, 7, 8	Thm. 1.6
12a ₁₇₃	169	$1 - 7t + 20t^2 - 35t^3 + 43t^4 - 35t^5 + 20t^6 - 7t^7 + t^8$	4	5, 6	Thm. 1.5
12a ₁₈₃	121	$6 - 30t + 49t^2 - 30t^3 + 6t^4$	5	5	Lem. 2.2
12a ₁₈₉	225	$1 - 8t + 26t^2 - 48t^3 + 59t^4 - 48t^5 + 26t^6 - 8t^7 + t^8$	4	6, 7, 8	Thm. 1.6
12a ₂₁₁	169	$2 - 8t + 20t^2 - 34t^3 + 41t^4 - 34t^5 + 20t^6 - 8t^7 + 2 * t^8$	5	5	Lem. 2.2
12a ₂₂₁	169	$2 - 14t + 40t^2 - 57t^3 + 40t^4 - 14t^5 + 2t^6$	4	5	Thm. 1.5
12a ₂₄₅	225	$1 - 7t + 24t^2 - 49t^3 + 63t^4 - 49t^5 + 24t^6 - 7t^7 + t^8$	4	6, 7, 8	Thm. 1.6
12a ₂₅₈	169	$1 - 7t + 20t^2 - 35t^3 + 43t^4 - 35t^5 + 20t^6 - 7t^7 + t^8$	4	5	Thm. 1.5
12a ₂₇₉	169	$2 - 15t + 40t^2 - 55t^3 + 40t^4 - 15t^5 + 2t^6$	5	5, 6	Lem. 2.2
12a ₃₇₇	225	$1 - 8t + 26t^2 - 48t^3 + 59t^4 - 48t^5 + 26t^6 - 8t^7 + t^8$	4	6, 7, 8	Thm. 1.6
12a ₄₂₅	81	$6 - 20t + 29t^2 - 20t^3 + 6t^4$	4	5	Thm. 1.5
12a ₄₂₇	225	$1 - 8t + 26t^2 - 48t^3 + 59t^4 - 48t^5 + 26t^6 - 8t^7 + t^8$	4	6	Thm. 1.6
12a ₄₃₅	225	$1 - 8t + 26t^2 - 48t^3 + 59t^4 - 48t^5 + 26t^6 - 8t^7 + t^8$	4	6	Thm. 1.6
12a ₄₄₇	121	$2 - 12t + 28t^2 - 37t^3 + 28t^4 - 12t^5 + 2t^6$	4	5	Thm. 1.5
12a ₄₅₆	225	$1 - 8t + 25t^2 - 48t^3 + 61t^4 - 48t^5 + 25t^6 - 8t^7 + t^8$	5	6, 7, 8	Thm. 1.6
12a ₄₅₈	289	$1 - 9t + 32t^2 - 63t^3 + 79t^4 - 63t^5 + 32t^6 - 9t^7 + t^8$	5	6, 7	Thm. 1.6
12a ₄₆₄	225	$1 - 7t + 24t^2 - 49t^3 + 63t^4 - 49t^5 + 24t^6 - 7t^7 + t^8$	4	6	Thm. 1.6
12a ₄₇₃	289	$1 - 8t + 30t^2 - 64t^3 + 83t^4 - 64t^5 + 30t^6 - 8t^7 + t^8$	5	6, 7	Thm. 1.6
12a ₄₇₇	169	$1 - 11t + 41t^2 - 63t^3 + 41t^4 - 11t^5 + t^6$	5	5	Lem. 2.2
12a ₄₈₄	289	$1 - 9t + 32t^2 - 63t^3 + 79t^4 - 63t^5 + 32t^6 - 9t^7 + t^8$	5	6	Thm. 1.6
12a ₆₀₆	169	$4 - 18t + 38t^2 - 49t^3 + 38t^4 - 18t^5 + 4t^6$	5	5	Lem. 2.2
12a ₆₃₁	225	$4 - 22t + 52t^2 - 69t^3 + 52t^4 - 22t^5 + 4t^6$	4	6	Thm. 1.6
12a ₆₄₆	169	$2 - 9t + 21t^2 - 33t^3 + 39t^4 - 33t^5 + 21t^6 - 9t^7 + 2t^8$	5	5, 6	Lem. 2.2
12a ₆₆₇	121	$2 - 7t + 15t^2 - 23t^3 + 27t^4 - 23t^5 + 15t^6 - 7t^7 + 2t^8$	5	5	Lem. 2.2
12a ₇₁₅	169	$4 - 18t + 38t^2 - 49t^3 + 38t^4 - 18t^5 + 4t^6$	5	5, 6	Lem. 2.2
12a ₇₈₆	169	$2 - 15t + 40t^2 - 55t^3 + 40t^4 - 15t^5 + 2t^6$	5	5, 6	Lem. 2.2
12a ₈₁₉	169	$1 - 5t + 12t^2 - 21t^3 + 29t^4 - 33t^5 + 29t^6 - 21t^7 + 12t^8 - 5t^9 + t^{10}$	5	5	Lem. 2.2
12a ₈₇₉	121	$2 - 7t + 15t^2 - 23t^3 + 27t^4 - 23t^5 + 15t^6 - 7t^7 + 2t^8$	5	5	Lem. 2.2
12a ₈₈₇	289	$1 - 9t + 32t^2 - 63t^3 + 79t^4 - 63t^5 + 32t^6 - 9t^7 + t^8$	5	6, 7	Thm. 1.6
12a ₉₇₅	225	$4 - 22t + 52t^2 - 69t^3 + 52t^4 - 22t^5 + 4t^6$	4	6	Thm. 1.6
12a ₉₇₉	225	$2 - 10t + 27t^2 - 46t^3 + 55t^4 - 46t^5 + 27t^6 - 10t^7 + 2t^8$	5	6, 7, 8	Thm. 1.6
12a ₁₀₁₁	121	$1 - 4t + 9t^2 - 15t^3 + 20t^4 - 23t^5 + 20t^6 - 15t^7 + 9t^8 - 4t^9 + t^{10}$	5	5	Lem. 2.2
12a ₁₀₁₉	361	$1 - 10t + 39t^2 - 80t^3 + 101t^4 - 80t^5 + 39t^6 - 10t^7 + t^8$	5	6	Thm. 1.6
12a ₁₀₂₉	81	$2 - 6t + 10t^2 - 14t^3 + 17t^4 - 14t^5 + 10t^6 - 6t^7 + 2t^8$	5	5	Lem. 2.2
12a ₁₀₃₄	121	$8 - 30t + 45t^2 - 30t^3 + 8t^4$	5	5	Lem. 2.2
12a ₁₀₈₃	169	$2 - 9t + 21t^2 - 33t^3 + 39t^4 - 33t^5 + 21t^6 - 9t^7 + 2t^8$	5	5, 6	Lem. 2.2
12a ₁₀₈₇	225	$1 - 8t + 25t^2 - 48t^3 + 61t^4 - 48t^5 + 25t^6 - 8t^7 + t^8$	5	6, 7, 8	Thm. 1.6
12a ₁₁₀₅	289	$1 - 8t + 30t^2 - 64t^3 + 83t^4 - 64t^5 + 30t^6 - 8t^7 + t^8$	5	6	Thm. 1.6
12a ₁₁₁₉	169	$2 - 9t + 21t^2 - 33t^3 + 39t^4 - 33t^5 + 21t^6 - 9t^7 + 2t^8$	5	5	Lem. 2.2
12a ₁₂₀₂	169	$9 - 42t + 67t^2 - 42t^3 + 9t^4$	5	5, 6	Lem. 2.2
12a ₁₂₆₉	169	$4 - 17t + 38t^2 - 51t^3 + 38t^4 - 17t^5 + 4t^6$	5	5	Lem. 2.2
12a ₁₂₇₇	121	$4 - 14t + 26t^2 - 33t^3 + 26t^4 - 14t^5 + 4t^6$	5	5	Lem. 2.2
12a ₁₂₈₃	81	$1 - 3t + 6t^2 - 10t^3 + 13t^4 - 15t^5 + 13t^6 - 10t^7 + 6t^8 - 3t^9 + t^{10}$	5	5	Lem. 2.2

TABLE 4. Symmetric ribbon number data and justifications for prime alternating symmetric ribbon knots with 12 crossings

K	$\det(K)$	$\Delta_K(t)$	$r(K) \geq$	$r_s(K) \geq$	lower
$11a_{103}$	81	$4 - 20t + 33t^2 - 20t^3 - 4t^4$	4	5	Thm. 1.5
$11a_{165}$	81	$2 - 9t + 18t^2 - 23t^3 + 18t^4 - 9t^5 + 2t^6$	4	5	Thm. 1.5
$11a_{201}$	81	$4 - 20t + 33t^2 - 20t^3 - 4t^4$	4	5	Thm. 1.5
$11n_{67}$	9	$2 - 5t + 2t^2$	3	4	Lem. 4.4
$11n_{73}$	9	$1 - 2t + 3t^2 - 2t^3 + t^4$	3	4	Lem. 4.4
$11n_{74}$	9	$1 - 2t + 3t^2 - 2t^3 + t^4$	3	4	Lem. 4.4
$11n_{97}$	9	$2 - 5t + 2t^2$	3	4	Lem. 4.4
$12a_{348}$	225	$2 - 17t + 54t^2 - 79t^3 + 54t^4 - 17t^5 + 2t^6$	5	6	Thm. 1.6
$12a_{990}$	225	$1 - 8t + 26t^2 - 48t^3 + 59t^4 - 48t^5 + 26t^6 - 8t^7 + t^8$	4	6	Thm. 1.6
$12a_{1225}$	225	$1 - 5t + 14t^2 - 28t^3 + 41t^4 - 47t^5 + 41t^6 - 28t^7 + 14t^8 - 5t^9 + t^{10}$	5	6	Thm. 1.6
$12n_{51}$	9	$2 - 5t + 2t^2$	3	4	Lem. 4.4
$12n_{56}$	9	$1 - 2t + 3t^2 - 2t^3 + t^4$	3	4	Lem. 4.4
$12n_{57}$	9	$1 - 2t + 3t^2 - 2t^3 + t^4$	3	4	Lem. 4.4
$12n_{62}$	81	$2 - 9t + 18t^2 - 23t^3 + 18t^4 - 9t^5 + 2t^6$	4	5	Thm. 1.5
$12n_{66}$	81	$2 - 9t + 18t^2 - 23t^3 + 18t^4 - 9t^5 + 2t^6$	4	5	Thm. 1.5

TABLE 5. Prime ribbon knots that are not known to admit symmetric union presentations. Note that the penultimate column is a lower bound for $r_s(K)$.

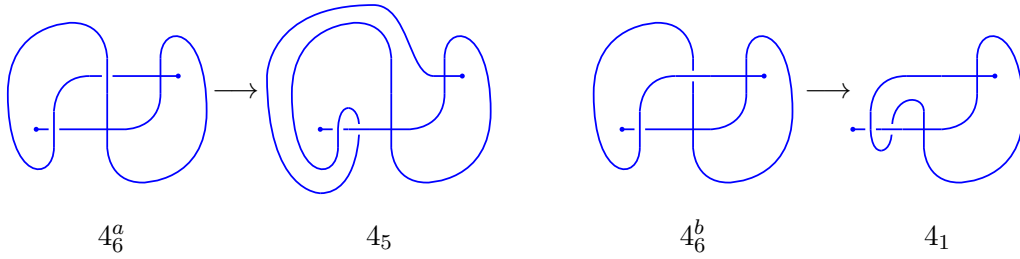


FIGURE 32. Two possible leaf isotopies on a labeled knotoid diagram of type 4_6 .

$$\begin{aligned}
 4_3 : & \quad 1 \\
 & \quad 1 - 3t^2 + t^4 \\
 & \quad 1 - t - t^2 + 3t^3 - t^4 - t^5 + t^6 \\
 & \quad 1 - 2t + 3t^2 - 4t^3 + 5t^4 - 4t^5 + 3t^6 - 2t^7 + t^8 \\
 & \quad 1 - 3t + 5t^2 - 7t^3 + 5t^4 - 3t^5 + t^6 \\
 & \quad 1 - 4t + 6t^2 - 8t^3 + 11t^4 - 8t^5 + 6t^6 - 4t^7 + t^8 \\
 & \quad 1 - 5t + 11t^2 - 15t^3 + 11t^4 - 5t^6 + t^6 \\
 & \quad 1 - 6t + 11t^2 - 6t^3 + t^4 \\
 & \quad 2 - 6t + 9t^2 - 6t^3 + 2t^4 \\
 & \quad 2 - 12t + 21t^2 - 12t^3 + 2t^4 \\
 & \quad 4 - 12t + 17t^2 - 12t^3 + 4t^4 \\
 & \quad 6 - 13t + 6t^2
 \end{aligned}$$

$$\begin{aligned}
4_4 : \quad & 1 \\
& 1 - 2t^2 + 3t^4 - 2t^6 + t^8 \\
& 1 - t - t^3 + 3t^4 - t^5 - t^7 + t^8 \\
& 1 - t + t^2 - 3t^3 + t^4 - t^5 + t^6 \\
& 1 - 2t + 3t^2 - 2t^3 + t^4 \\
& 1 - 2t + 3t^2 - 4t^3 + 5t^4 - 4t^5 + 3t^6 - 2t^7 + t^8 \\
& 1 - 3t + 5t^2 - 7t^3 + 5t^4 - 3t^5 + t^6 \\
& 1 - 6t + 11t^2 - 6t^3 + t^4 \\
& 2 - 5t^2 + 2t^4 \\
& 2 - 5t + 2t^2 \\
& 2 - 6t + 9t^2 - 6t^3 + 2t^4 \\
& 6 - 13t + 6t^2
\end{aligned}$$

$$\begin{aligned}
4_7 : \quad & 1 \\
& 1 - 2t^2 + 3t^4 - 2t^6 + t^8 \\
& 1 - t - t^3 + 3t^4 - t^5 - t^7 + t^8 \\
& 1 - t - t^2 + 3t^3 - t^4 - t^5 + t^6 \\
& 1 - t + t^2 - 3t^3 + t^4 - t^5 + t^6 \\
& 1 - 2t + t^2 + 2t^3 - 5t^4 + 2t^5 + t^6 - 2t^7 + t^8 \\
& 1 - 2t + 3t^2 - 2t^3 + t^4 \\
& 1 - 3t - t^2 + 7t^3 - t^4 - 3t^5 + t^6 \\
& 1 - 3t + 6t^2 - 9t^3 + 11t^4 - 9t^5 + 6t^6 - 3t^7 + t^8 \\
& 1 - 5t + 11t^2 - 15t^3 + 11t^4 - 5t^6 + t^6 \\
& 2 - 5t^2 + 2t^4 \\
& 2 - 3t - 2t^2 + 7t^3 - 2t^4 - 3t^5 + 2t^6 \\
& 2 - 5t + 2t^2 \\
& 2 - 6t + 10t^2 - 13t^3 + 10t^4 - 6t^5 + 2t^6 \\
& 2 - 12t + 21t^2 - 12t^3 + 2t^4 \\
& 3 - 12t + 19t^2 - 12t^3 + 3t^4 \\
& 4 - 12t + 17t^2 - 12t^3 + 4t^4
\end{aligned}$$

$$\begin{aligned}
4_8 : & \quad 1 \\
& \quad 1 - 2t^2 + 3t^4 - 2t^6 + t^8 \\
& \quad 1 - t - t^2 + 3t^3 - t^4 - t^5 + t^6 \\
& \quad 1 - t - 3t^2 + 7t^3 - 3t^4 - t^5 + t^6 \\
& \quad 1 - 2t + 4t^3 - 7t^4 + 4t^5 - 2t^7 + t^8 \\
& \quad 1 - 2t + t^2 + 2t^3 - 5t^4 + 2t^5 + t^6 - 2t^7 + t^8 \\
& \quad 1 - 2t + 3t^2 - 2t^3 + t^4 \\
& \quad 1 - 3t - t^2 + 7t^3 - t^4 - 3t^5 + t^6 \\
& \quad 2 - 5t^2 + 2t^4 \\
& \quad 2 - 3t - 2t^2 + 7t^3 - 2t^4 - 3t^5 + 2t^6 \\
& \quad 2 - 5t + 2t^2
\end{aligned}$$

These lists contain a total of 27 distinct Alexander polynomials, which are sorted by determinant in Table 1. \square

REFERENCES

- [AAC⁺25] Xianhao An, Matthew Aronin, David Cates, Ansel Goh, Benjamin Kirn, Josh Krienke, Minyi Liang, Samuel Lowery, Ege Malkoc, Jeffrey Meier, Max Natanson, Veljko Radić, Yavuz Rodoplu, Bhaswati Saha, Evan Scott, Roman Simkins, and Alexander Zupan, *Ribbon numbers of 12-crossing knots*, J. Knot Theory Ramifications **34** (2025), no. 13, Paper No. 2550066, 45. MR 4978631
- [Ace14] Paolo Aceto, *Symmetric ribbon disks*, J. Knot Theory Ramifications **23** (2014), no. 9, 1450048. MR 3268984
- [CDGW] Marc Culler, Nathan M. Dunfield, Matthias Goerner, and Jeffrey R. Weeks, *SnapPy, a computer program for studying the geometry and topology of 3-manifolds*, Available at <http://snappy.computop.org>.
- [Eis09] Michael Eisermann, *The Jones polynomial of ribbon links*, Geom. Topol. **13** (2009), no. 2, 623–660. MR 2469525
- [EL07] Michael Eisermann and Christoph Lamm, *Equivalence of symmetric union diagrams*, J. Knot Theory Ramifications **16** (2007), no. 7, 879–898. MR 2354266
- [FMZ24] Stefan Friedl, Filip Misev, and Alexander Zupan, *Bounding the ribbon numbers of knots and links*, arXiv e-prints (2024), arXiv:2408.11618, To appear in Alg. & Geom. Top.
- [GDS19] Dimos Goundaroulis, Julien Dorier, and Andrzej Stasiak, *A systematic classification of knotoids on the plane and on the sphere*, arXiv e-prints (2019), arXiv:1902.07277.
- [Kid87] Mark E. Kidwell, *On the degree of the Brandt-Lickorish-Millett-Ho polynomial of a link*, Proc. Amer. Math. Soc. **100** (1987), no. 4, 755–762. MR 894450
- [Lam00] Christoph Lamm, *Symmetric unions and ribbon knots*, Osaka J. Math. **37** (2000), no. 3, 537–550. MR 1789436
- [Lam21a] ———, *The search for nonsymmetric ribbon knots*, Exp. Math. **30** (2021), no. 3, 349–363. MR 4309311
- [Lam21b] ———, *Symmetric union presentations for 2-bridge ribbon knots*, J. Knot Theory Ramifications **30** (2021), no. 12, Paper No. 2141009, 11. MR 4394065
- [LM26] Charles Livingston and Allison H. Moore, *Knotinfo: Table of knot invariants*, URL: knotinfo.org, April 2026.
- [Miz06] Yoko Mizuma, *An estimate of the ribbon number by the Jones polynomial*, Osaka J. Math. **43** (2006), no. 2, 365–369. MR 2262340
- [Mur87] Kunio Murasugi, *Jones polynomials and classical conjectures in knot theory*, Topology **26** (1987), no. 2, 187–194. MR 895570
- [Sto03] A. Stoimenow, *The crossing number and maximal bridge length of a knot diagram*, Pacific J. Math. **210** (2003), no. 1, 189–199, With an appendix by Mark Kidwell. MR 1989075

- [The21] The Sage Developers, *Sagemath, the Sage Mathematics Software System (Version 10.2)*, 2021, <https://www.sagemath.org>.
- [Thi87] Morwen B. Thistlethwaite, *A spanning tree expansion of the Jones polynomial*, *Topology* **26** (1987), no. 3, 297–309. MR 899051

DEPARTMENT OF PHYSICS AND ASTRONOMY, UNIVERSITY OF NEBRASKA–LINCOLN, LINCOLN, NE 68588
Email address: `sakash2@huskers.unl.edu`

DEPARTMENT OF MATHEMATICS, UNIVERSITY OF NEBRASKA–LINCOLN, LINCOLN, NE 68588
Email address: `ericanthonycorrado@gmail.com`

DEPARTMENT OF MATHEMATICS, UNIVERSITY OF NEBRASKA–LINCOLN, LINCOLN, NE 68588
Email address: `bplacke4@huskers.unl.edu`

DEPARTMENT OF MATHEMATICS, UNIVERSITY OF NEBRASKA–LINCOLN, LINCOLN, NE 68588
Email address: `ssanketh2@huskers.unl.edu`

DEPARTMENT OF MATHEMATICS, UNIVERSITY OF NEBRASKA–LINCOLN, LINCOLN, NE 68588
Email address: `nickstarns.cs@gmail.com`

DEPARTMENT OF MATHEMATICS, UNIVERSITY OF NEBRASKA–LINCOLN, LINCOLN, NE 68588
Email address: `atimothy3@huskers.unl.edu`

DEPARTMENT OF MATHEMATICS, UNIVERSITY OF NEBRASKA–LINCOLN, LINCOLN, NE 68588
Email address: `zupan@unl.edu`
URL: <https://math.unl.edu/azupan2>